A Modular Treatment of Molecular Traffic Through the Active Site of Cholinesterase

Simone A. Botti*#, Clifford E. Felder*, Shneior Lifson§, Joel L. Sussman* and Israel Silman#
Departments of *Structural Biology, #Neurobiology, and §Chemical Physics Weizmann Institute of Science, Rehovot 76100, Israel

ABSTRACT We present a model for the molecular traffic of ligands, substrates, and products through the active site of cholinesterases (ChEs). First, we describe a common treatment of the diffusion to a buried active site of cationic and neutral species. We then explain the specificity of ChEs for cationic ligands and substrates by introducing two additional components to this common treatment. The first module is a surface trap for cationic species at the entrance to the active-site gorge that operates through local, short-range electrostatic interactions and is independent of ionic strength. The second module is an ionic-strength-dependent steering mechanism generated by long-range electrostatic interactions arising from the overall distribution of charges in ChEs. Our calculations show that diffusion of charged ligands relative to neutral isosteric analogs is enhanced ~10-fold by the surface trap, while electrostatic steering contributes only a 1.5- to 2-fold rate enhancement at physiological salt concentration. We model clearance of cationic products from the active-site gorge as analogous to the escape of a particle from a one-dimensional well in the presence of a linear electrostatic potential. We evaluate the potential inside the gorge and provide evidence that while contributing to the steering of cationic species toward the active site, it does not appreciably retard their clearance. This optimal fine-tuning of global and local electrostatic interactions endows ChEs with maximum catalytic efficiency and specificity for a positively charged substrate, while at the same time not hindering clearance of the positively charged products.

INTRODUCTION

Cholinesterases (ChEs) are a family of enzymes that fall broadly into two types: acetylcholinesterase (AChE) and butyrylcholinesterase (BChE). They are distinguished primarily by their substrate specificity: AChE hydrolyzes the natural neurotransmitter acetylcholine (ACh) faster than choline esters with bulkier acyl chains; thus it is much less active on the synthetic substrate, butyrylcholine (BCh). In contrast, BChE displays similar activity toward the two substrates (Chatonnet and Lockridge, 1989).

Vertebrates contain both AChE and BChE, which probably originate from the duplication of a single ChE gene (Massoulié et al., 1993). Insects possess a single ChE gene coding for an enzyme with a specificity intermediate between those of AChE and BChE (Massoulié et al., 1993; Taylor and Radic, 1994), while in certain nematode species, up to four ChE genes have been identified (Grauso et al., 1998). The principal physiological function of AChE has long been known to be termination of impulse transmission at cholinergic synapses by rapid hydrolysis of ACh, but the biological role of BChE is still an open question (Chatonnet and Lockridge, 1989).

ChEs are able to catalyze the rapid breakdown of a variety of esters, both cationic and neutral (Quinn, 1987). The highest catalytic rate is displayed by AChE hydrolysis of ACh, at a rate approaching the diffusion-controlled limit (Rosenberry, 1975b; Hasinoff, 1982; Bazelyansky et al., 1986). This efficiency is a common characteristic of ChEs. A tally of the bimolecular rate constants (k_{cat}/K_M) among ChEs for their best substrates shows a spread of less than an order of magnitude. Values range from $1.6 \times 10^8\ M^{-1}\ s^{-1}$, for hydrolysis of ACh by *Electrophorus electricus* AChE (*Ee*AChE) (Rosenberry, 1975a), to $4.0 \times 10^7\ M^{-1}\ s^{-1}$ for BChE hydrolysis of both ACh and BCh (Vellom et al., 1993).

Catalytic efficiency of ChEs for neutral substrates is also very high. Values of k_{cat}/K_M for hydrolysis by AChE of ACh and of its neutral isoster 3,3-dimethylbutylacetate (DBA) do differ by ~40-fold at physiological salt concentration (Hasan et al., 1981), but there is evidence that the hydrolysis of the thio analog of DBA is also diffusion-controlled (Bazelyansky et al., 1986). Moreover, it has been shown that BChE turns over *o*-nitrophenyl butyrate (*o*-NPB) faster than it breaks down butyrylthiocholine (Masson et al., 1997).

Studies of the pH and charge dependence of catalytic hydrolysis of substrates and of binding of reversible inhibitors suggested that the active site of ChEs contains two major subsites, the "esteratic" and the "anionic" (Wilson and Bergmann, 1950), corresponding, respectively, to the catalytic machinery and the choline-binding pocket (Froede and Wilson, 1971). The high bimolecular association constants for cationic ligands and their ionic strength dependence suggested a high charge density in the active site. This led to the prediction that up to nine negative charges were present in the "anionic" site (Rosenberry and Neumann, 1977; Nolte et al., 1980). A second "anionic" site, which became known as the "peripheral" anionic site (PAS), was proposed based on binding of bis-quaternary

Received for publication 4 September 1998 and in final form 23 July 1999.
Address reprint requests to Dr. Simone A. Botti, Department of Structural Biology, Weizmann Institute of Science, 76100 Rehovot, Israel. Tel.: 972-8-934-3759; Fax: 972-8-934-4159; E-mail: simone.botti@weizmann.ac.il.

0006-3495/99/11/2430/21 $2.00

ammonium compounds (Bergmann et al., 1950). Binding of ligands to the peripheral anionic site causes inactivation of the enzyme, though the mechanism of inhibition is not clear. It has been speculated that the PAS is involved in the phenomenon of substrate inhibition and activation through binding of a second substrate molecule. Its function may involve either allosteric modification of the active site (Radic et al., 1991; Shafferman et al., 1992; Barak et al., 1995) or alteration of the traffic of substrate and products by blocking access to the catalytic machinery (Berman and Nowak, 1992; Haas et al., 1992; Schalk et al., 1992). In addition, there is evidence for an involvement of the PAS in functions distinct from catalysis. Recent studies have presented evidence for a role of the PAS of AChE in neurite regeneration and outgrowth (Layer et al., 1993; Willbold and Layer, 1994; Jones et al., 1995; Srivatsan and Peretz, 1997) and in the growth and differentiation of spinal motor neurons (Bataillé et al., 1998).

Catalysis by ChEs occurs by a mechanism similar to that of the serine proteases, via an acyl-enzyme intermediate. It is assumed to involve a tetrahedral transition state produced by nucleophilic attack on the substrate by a serine, followed by general-base catalysis assisted by a histidine. The transition state subsequently collapses to the acyl-enzyme by general-acid-catalyzed expulsion of choline (Quinn, 1987). Solution of the three-dimensional (3D) structure of AChE from *Torpedo californica* (*Tc*AChE) (Sussman et al., 1991) was followed by determination of the crystal structures of several complexes of AChE with specific inhibitors (Harel et al., 1993, 1995, 1996). Analysis of these structures, taken together with systematic site-directed mutagenesis studies (Radic et al., 1991, 1993; Shafferman et al., 1992; Barak et al., 1995), has permitted identification of the key functional residues in the active site and contributed to clarification of their role in recognition of substrates and inhibitors. (A comprehensive and updated list of references for cholinesterase mutants can be obtained through the ESTHER server, http://meleze.ensam.inra.fr/cholinesterase (Cousin et al., 1997).) It has thus been possible to construct a picture of the structural factors governing both the mechanism and specificity of ChEs. At the same time the data obtained have given rise to a new set of still unanswered questions.

The structure/function relationships that have emerged over the past seven years paint a picture of a family of rapid enzymes specific for cationic substrates that have evolved to very high catalytic efficiency by adopting some rather counterintuitive solutions. The active-site serine of *Tc*AChE, S200, was unexpectedly found to be located near the bottom of a 24-Å-deep gorge, ~4.4 Å wide at its narrowest point and 8.0 Å wide at its mouth. This serine forms a catalytic triad with H440 and E327. [Residue numbers follow the guidelines established at the 1992 OHOLO meeting, Eilat (Massoulié et al., 1993). The numbering used is that of the sequence of *Tc*AChE. When species-specific numbers are employed, the homologous position in *Tc*AChE will follow, printed in italics and appearing in parentheses.] Contrary to the assumption of a concentration of negative charges within the active site (Nolte et al., 1980), no more than two formal negative charges were found near the active site serine (E199 and E443). In fact, the walls of the gorge were found to be lined by the side-chains of 14 conserved aromatic residues (Sussman et al., 1991). In analogy to studies of ACh binding to model hosts (Dougherty and Stauffer, 1990), it was suggested that the binding of ACh to the sites within the gorge involved in substrate recognition is stabilized by interactions between the quaternary ammonium group of ACh and the π electrons of some of the conserved aromatic residues of AChE. This hypothesis was confirmed by inspection of the structures of complexes of AChE with various quaternary inhibitors (Harel et al., 1993). Analysis of the 3D structure of the complex of AChE with the transition-state analog, *m*-trimethylammonium trifluoroacetophenone (TFK^+), has highlighted the specific intermolecular interactions between the substrate and the active site that are responsible for the catalytic efficacy of AChE. These structural data suggest that the particular active-site configuration of AChE allows the enzyme to efficiently sequester the acylation transition state in a preorganized polar environment formed by the oxyanion hole, consisting of the main-chain N-H dipoles, G118, G119, and A201, and the side chains of key aromatic residues such as W84 and F330 (Harel et al., 1996). This environment is able to stabilize the catalytic transition state by providing it with larger electrostatic stabilization than in the solvent and is the basis of the catalytic power of the ChEs (Fuxreiter and Warshel, 1998).

Inspection of the overall 3D structure of *Tc*AChE revealed a marked asymmetrical surface distribution of charged residues. These residues were shown to segregate roughly into a "northern" negative hemisphere, considering the mouth of the gorge as the north pole, and a "southern" positive one, giving rise to a large "dipole moment" roughly oriented along the axis of the active-site gorge (Ripoll et al., 1993; Tan et al., 1993; Antosiewicz et al., 1994; Felder et al., 1997). The magnitude of this "dipole moment" was estimated, by electrooptical measurements on *Bungarus fasciatius* AChE (*Bf*AChE), to be ~1000 Debyes (Porschke et al., 1996). The biological significance of these unusual electrostatic properties has been the subject of much controversy. It has been suggested that the "macrodipole" might act to steer cationic ligands to the mouth of the gorge (Sussman et al., 1991; Tan et al., 1993), where they would bind to the aromatic residues lining it and subsequently be committed to moving down the gorge, toward the active site, in a fashion similar to that of an affinity column (Sussman et al., 1991). Calculations of the rates of encounter of charged ligands and substrates based on Brownian dynamics (BD) simulations predicted that the electrostatic properties of AChE would be responsible for a rate enhancement of up to 240-fold (Zhou et al., 1996). The possibility of a large electrostatic steering effect on positively charged substrates has raised the question of the route of clearance of choline (Ch), the cationic product of enzy-

matic hydrolysis, which would seem to be trapped at the bottom of the gorge by a strong electric field.

Molecular dynamics (MD) simulations have suggested that an alternative route of access to the active site might open via the concerted movement of residues W84, V129, and G441 (Gilson et al., 1994), while a more recent MD study has identified a number of "side entrances" to the gorge, all involving concerted movements of a number of side chains in the Ω loop (C67–C92) of AChE (Wlodek et al., 1997b). As yet, no simple and predictive model for the clearance of the products of hydrolysis of ACh or BCh has been introduced into the treatment of the molecular traffic of substrates and ligands through the active site of ChEs.

The importance of electrostatic interactions in the steering of cationic substrates to the active site of ChEs was challenged by a study of a series of mutants of human recombinant AChE (hAChE), in which up to seven negative residues around the outer rim of the gorge were neutralized, thus substantially reducing the magnitude of the "macrodipole," without producing large changes in the second-order hydrolysis rate constant (Shafferman et al., 1994). The contradiction between data documenting the electrostatic properties of ChEs and the apparent lack of correlation between their experimental modification and a major catalytic effect has been the topic of various studies. Antosiewicz and co-workers (Antosiewicz et al., 1994, 1995a,b, 1996; Antosiewicz and McCammon, 1995) have attempted to correlate the electrostatic properties of AChE with the on rates for charged ligands and the second-order hydrolysis rate constants. The picture emerging from their work supports the existence of an electrostatic steering effect in ChEs. Moreover, calculations performed by the same group, on structural models of the mutants analyzed kinetically by Shafferman et al. (1994), account for the small changes in catalytic rates observed. This reconciles the hypothesis of a role for electrostatics in accelerating the encounter between the enzyme and reactive species with experimental data that seemed to argue against it (Antosiewicz et al., 1995b). Nevertheless, these studies were unable to strongly correlate experimental results with any one particular aspect of the electrostatic properties of the ChEs, since neither the total charge nor the dipole moment fully accounted for the electrostatic steering of ligand to the active site.

Calculations of the potential gradient along the axis of the gorge and of its dependence on salt concentration have been performed both for wild-type (WT) AChE of different species and for a series of surface and active-site mutants (Antosiewicz et al., 1995b; Wlodek et al., 1997a; Felder et al., 1997). These calculations have revealed that AChEs display a similar negative potential gradient, beginning several angstroms outside the gorge entrance, and continuing down the gorge toward the active site. This potential is not correlated with ChE surface charge distribution, but is due to a combined effect of the overall charge distribution in the ChE molecule, including the effect of several α-helix dipoles. The results of these studies suggest the existence of a long-range electrostatic interaction, attributable to this potential gradient, that contributes to both the enhancement of encounter rates between cationic ligands and the catalytic machinery buried at the bottom of the active-site gorge of ChEs. Radic et al. (1997) have performed a detailed analysis of the influence of electrostatics on the kinetics of ligand binding to AChE. This study focused on the ionic-strength dependence of the binding of reversible inhibitors to AChE after neutralization, by site-directed mutagenesis, of anionic side chains in the surface area around the entrance to the active-site gorge, in the PAS and in the active center. Comparison of the experimental data to BD simulations of the on rates of the ligands revealed good agreement for surface mutants, while predictions were less accurate when some key residues in the PAS were neutralized. The results were interpreted in the framework of two distinct types of electrostatic interactions: the first, dependent on salt concentration, causing acceleration of the initial encounter rates of cationic ligands with the enzyme, and the second, independent of salt concentration, resulting in trapping of these ligands by specific residues in the PAS or within the active site. The presence of a trap for cationic ligands in AChE and BChE has been proposed in several other studies (Rosenberry and Neumann, 1977; Hasinoff, 1982; Hosea et al., 1996; Masson et al., 1996, 1997), but no analytical and quantitative treatment of the effect of a trapping surface on the encounter rate of cationic ligands with the ChEs has been advanced until now.

In the following sections we will present a model for the molecular traffic of neutral and cationic ligands, substrates, and products through the active site of ChEs, and we will evaluate the contributions of electrostatic interactions to the traffic of cationic species.

First, we will illustrate a common treatment for the diffusion of both neutral and cationic ligands toward an enzyme characterized by a buried active site. Subsequently, we will show how the specificity of ChEs for cationic ligands and substrates can be treated by introducing two additional modules to this common treatment:

1. A module that incorporates the effects of short-range and ionic strength *independent* interactions between key residues in the area of the entrance to the active-site gorge and the quaternary ammonium moiety of cationic substrates and ligands. This local module will be shown to describe the effects of a putative trapping mechanism for cationic species. The effect of this surface trap on the enhancement of encounter rates between cationic ligands and ChEs will be analyzed quantitatively by correlating the electrostatic potentials in the area surrounding the entrance to the active-site gorge with the experimentally measured encounter rates of cationic ligands with ChEs.
2. A module that incorporates the effects of long-range and ionic-strength *dependent* interactions. This global module, which is shown to describe the steering of cationic substrates and ligands to the gorge floor, can be analyzed quantitatively by evaluating the overall electric potential

around the entrance and within the active-site gorge and its dependence on ionic strength.

The clearance of positively charged products and ligands from the active-site gorge will be considered as analogous to the Brownian migration of a charged particle out of a one-dimensional box against an electrostatic potential linear in distance along the length of the box. For neutral molecules, the value of this potential will be set to zero, while for charged species we will introduce values of the gorge potential either derived from experimental data or calculated with the Poisson-Boltzmann equation (PB).

This modular approach will enable us to rationalize the apparent paradox of electric fields, which act to steer cationic species toward the active site while at the same time not hindering the clearance of positively charged products. The results obtained will be used to discuss the mechanisms involved in the emergence of the specificity of ChEs for cationic substrates from the framework of an already very efficient catalytic machinery for the hydrolysis of small esters.

METHODS: ELECTROSTATIC CALCULATIONS AND HOMOLOGY MODELS

We calculated the electrostatic potential along the active-site gorge of ChEs, by solving the PB equation, to study the influence on gorge electrostatic potentials of salt concentration and of the neutralization of a number of key residues in the area of the surface cationic trap and in the active-site gorge. The electrostatic calculations were performed on the following enzymes (where crystallographic coordinates are available, the PDB ID code will follow in parentheses): AChE from the following species: *Torpedo californica* (*Tc*AChE-PDB ID: 2ACE), mouse (mAChE-PDB ID 1MAH), *Bungarus fasciatus* (*Bf*AChE), *Drosophila melanogaster* (*Dm*AChE), and human (hAChE); and human BChE (hBChE). Where the crystallographic coordinates were not available, homology models were constructed. The residues to be mutated were chosen on the basis of their presumed involvement in the recognition of cationic substrates and in the contribution to the steering of cationic ligands toward the active site of ChEs (Shafferman et al., 1992, 1994; Radic et al., 1993, 1995; Barak et al., 1995; Masson et al., 1996; Ordentlich et al., 1996). Three classes of mAChE mutants, as shown in Table 1, were generated by homology modeling from the respective WT structures. The positions of these mutations on the 3D fold of ChE are illustrated in Fig. 1. In the first class, based on the studies of Shafferman et al. (1994) and Radic et al. (1997), we generated five mutant structures in which up to seven acidic residues on the enzyme surface near the gorge entrance were neutralized. In the second and third classes, the mutations focused on the modification of residues in the area of the cationic trap and at the bottom of the gorge, respectively, to analyze the correlation between local and overall electrostatic potentials and the encounter rates of cationic ligands and substrates.

Construction of homology models

In brief, models were constructed by use of the automated knowledge-based model-building tool resident on the Swiss-Model Server (Peitsch, 1996) (http://www.expasy.ch/swissmod/SWISS_MODEL.html), employing 3D structures of *Tc*AChE (PDB ID 2ACE, 1ACJ, 1FSS) and mAChE (PDB ID 1MAH) as templates. The automatic procedure involved alignment of the sequence to be modeled with the template sequences, by application of the BLAST algorithm (Altschul et al., 1990). Regions of sequence similarity were automatically selected and employed to build a framework for the model structure. Missing loops were automatically constructed by searching the PDB database, employing either the best fitting fragment corresponding to the sequence or a framework constructed by the average of the five best fragments. The last step of the procedure involved automated rebuilding of side chains, verification of the quality of the model, and refinement of the final structure by energy minimization and molecular dynamics. The models were then checked again manually, and any missing part that was not successfully built automatically was added manually as described previously (Felder et al., 1997).

TABLE 1 List of mAChE mutants employed in this study

mAChE surface mutants
D275V (*D280V*)
D275V/D278N (*D280V/D283N*)
E82Q/E89Q/D275V/D278N (*E84Q/E91Q/D280V/D283N*)
E82Q/E89Q/D275V/D278N/D365N (*E84Q/E91Q/D280V/D283N/E372N*)
E82Q/E89Q/D275V/D278N/E285Q/D365N (*E84Q/E91Q/D280V/D283N/E292Q/E372N*)
mAChE trap mutants
D72N (*D74N*)
D72N/D275V/D278N (*D74N/D280V/D283N*)
mAChE gorge mutant
E199Q (*E202Q*)

*Tc*AChE numbering is employed. The mAChE numbering follows in parentheses and italics.

Calculation of electrostatic potentials along the active-site gorge

The electrostatic potential along the active-site gorge was calculated by generating a string of dummy atoms at 1-Å intervals along the gorge axis (Fig. 1) and evaluating the electric potential for the position of each dummy atom. The axis of the active-site gorge in the structures examined was defined as extending from atom I444-CD (gorge bottom) to the center of mass of atoms E73-CA, N280-CB, D285-CG, and L333-O (gorge entrance) (Antosiewicz and McCammon, 1995). The portion of the gorge extending from the bottom to S200-OG was defined as the binding region (~4 Å long), and the remainder as the transit region (~20 Å long). The width of the gorge mouth was measured by taking the average of the values of gorge radii originating from the center of mass of atoms E73-CA, N280-CB, D285-CG, and L333-O and intersecting the gorge rim at the CB atoms of residues D72, W279, D273, and D365. To study the local electrostatic potentials generated in the gorge by the residues involved in the cationic trap, we defined a region of the gorge extending from its mouth (as defined above) to a depth of 6 Å. The value of the electrostatic potential along this portion of the axis was then averaged and taken as a measure of the local potential in the trap region.

The PB equation was solved by the finite-difference method (Warwicker and Watson, 1982), using the QDIFFXS algorithm of version 3.0 of DelPhi (Gilson and Honig, 1988; Honig and Nicholls, 1995). A grid of up to 90 $Å^3$ was used. Calculations were performed, using an initial coarser grid with a 35-Å border and 1.45-Å grid spacing and subsequently focusing onto a second grid with a 10-Å border and 0.89-Å spacing. The internal and external dielectric constants were fixed at values of 2 and 80, respectively. Calculations were performed for salt concentrations of 5, 145, and 670 mM. The Stern ion exclusion layer was set at 2 Å, and the dielectric boundary between protein and solvent was constructed using a probe radius of 1.4 Å. Calculations were performed at 298.15 K and pH 7.0, using the Parse partial atomic charge and radius set (Sitkoff et al., 1994). The protonation states of the ionizable amino acids were assigned by examination of the solvent accessibility of their side chains in the 3D structure.

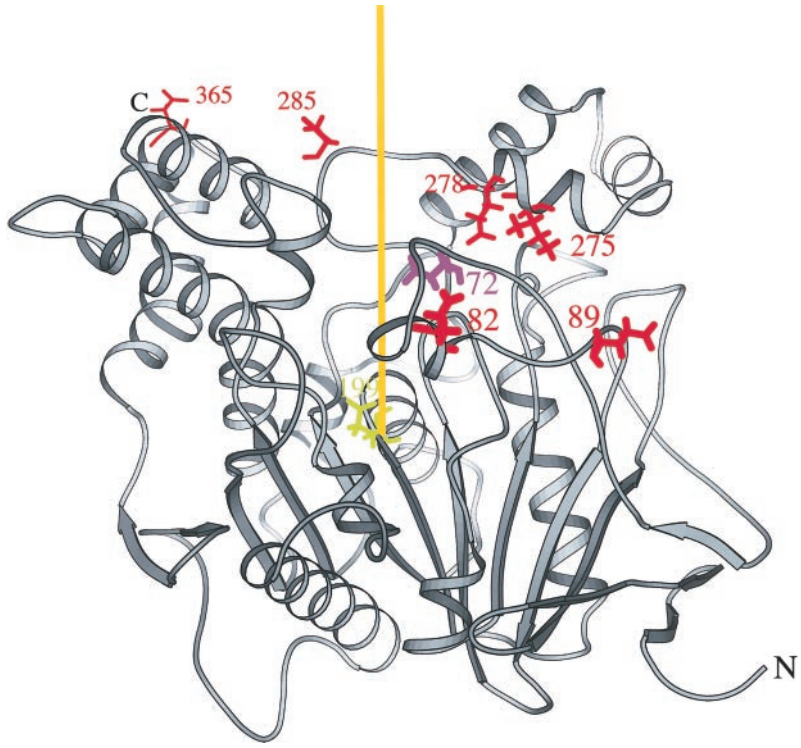

FIGURE 1 Ribbon diagram of AChE showing the relative positions of the mutated residues. The axis of the gorge is indicated by the yellow bar; the side chains of the surface mutants are colored in red; E199, at the bottom of the gorge, is in green; and D72, the main component of the cationic trap, is in purple.

On the basis of this analysis, all Glu, Asp, Lys, and Arg residues were set to be fully ionized, and the average charge on the active-site H440 and on all other histidines was set to zero (M. K. Gilson, personal communication). Potential values are expressed in kT/e units (1 kT/e = 25.6 mV = 0.593 kcal/mol/e).

RESULTS AND DISCUSSION

Because our study focuses on providing a model for the diffusive and binding events occurring before and after the bond rearrangement and cleavage steps of catalysis, the experimental parameters best suited for comparison with our model are the on rates and binding constants (k_{on} and K_i) of transition-state analogs, whose magnitudes are dependent only on the processes of diffusion and binding to the active site of ChEs. The contributions of both long- and short-range electrostatic interactions to the stability of the complex formed between a charged transition-state analog and AChE (or BChE) and to the on rate of the ligand can be evaluated by comparing the values of K_i and k_{on} for the charged species with those for a neutral isosteric ligand. These results can then be used to segregate the contributions of electrostatic interactions to molecular traffic from their effect on the chemical steps of catalysis.

Peptidyl trifluoromethyl ketones have been used extensively as transition-state analogs of various serine hydrolases (Imperiali and Abeles, 1986; Takahashi et al., 1988; Allen and Abeles, 1989b; Brady et al., 1989). In particular, they have been employed to assess the role of global electrostatic interactions in the stabilization of the catalytic transition state of subtilisin BPN′ (Jackson and Fersht, 1993). A large body of kinetic evidence demonstrates that another series of trifluoromethyl ketones serves as transition-state analogs of ChEs (Allen and Abeles, 1989a; Nair et al., 1993, 1994). The structure of the complex of the phenyl trifluoromethyl ketone, TFK^+, with *Tc*AChE has been solved by x-ray crystallography, illustrating in detail the structural interactions responsible for the tight binding of this particular transition-state analog (Harel et al., 1996). The effect of salt concentration and of the mutation of residues D72, E199, and several negatively charged surface residues on the K_i of both TFK^+ and its isosteric neutral analog, *m*-tertbutyltrifluoroacetophenone (TFK^0) (Quinn et al., 1995; Radic et al., 1995, 1997; Hosea et al., 1996), have been measured.

Accordingly, the results of our calculations, presented in the following sections, will be compared to experimental data collected for TFK^+, TFK^0, and another ligand, *N*-methylacridinium (NMA), which has been employed to study the role of electrostatic properties in ChE catalysis (Nolte et al., 1980).

Part I: Molecular traffic—diffusion

A common treatment for the diffusion of cationic and neutral isosteric ligands to a buried active site points toward two different limits for diffusion to the active site of ChEs

In treating the diffusion of ligands and substrates toward ChEs, we will employ the model described by Samson and Deutch (1978). In this model, the enzyme is approximated as a sphere, and the active site by a spherical cap. It focuses on the effect of burying a reactive site on the inside of an

enzyme, away from the surface and at the bottom of a conical duct. The rest of the spherical surface, including the walls of the duct, is considered to be inert. The relationship between the actual 3D structure of AChE and the model is shown in Fig. 2. The entrance to the active-site gorge constitutes a cap on the surface of a sphere of radius R. The gorge is modeled as a conical duct, characterized by an opening angle, ϑ. The bottom of this duct is delimited by a spherical cap of radius ρ, the surface of which includes the catalytic machinery of the enzyme. We will ignore complications arising from hydrodynamic interactions and dynamic conformational changes of the enzyme. BD simulations of the diffusion of a ligand to the active site of AChE indicate that the influence of these effects on the diffusive process is not very significant (Antosiewicz et al., 1995a; Antosiewicz and McCammon, 1995).

The following expressions should permit evaluation of the upper limit for the encounter rates of charged and neutral ligands without postulating any special diffusive mechanism for cationic species. According to Samson and Deutch (1978), the rate constant for the encounter of a ligand with the active site buried at the bottom of the conical duct can be expressed as

$$k(\vartheta, s) = 4\pi DR\frac{1}{2}[1 - \cos\vartheta]\left[\left(\frac{1-s}{s}\right) + \eta(\cos\vartheta)\right]^{-1} \quad (1)$$

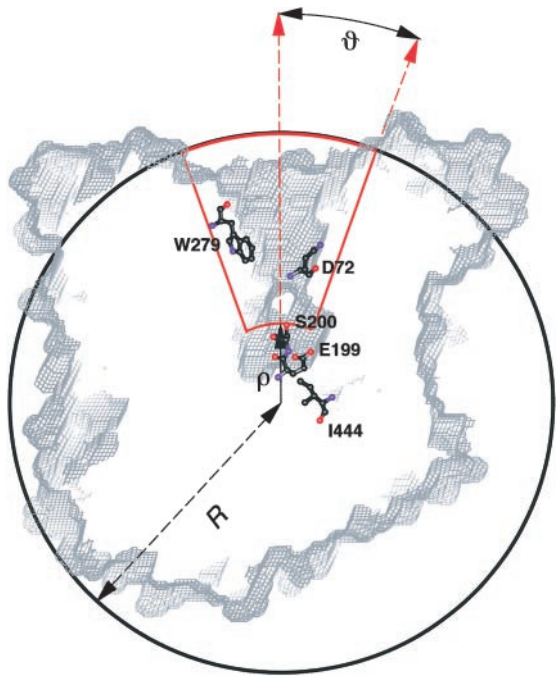

FIGURE 2 Schematic diagram of the model for diffusion of neutral and cationic ligands and substrates to the active site of ChE. The spherical model is superimposed on a slab view of *Tc*AChE showing the active-site gorge and the positions of D72 and of the catalytic serine, S200. The inner and outer spherical caps are colored in red. The inner cap includes the catalytic machinery of AChE, as can be seen by the position of S200.

where s is given by ρ/R, D is the diffusion coefficient of the ligand, and the function $\eta(\cos\vartheta)$ is given by the following expression:

$$\eta(x) = \frac{1}{2}\left[(1-x) + \sum_{l=1}^{\infty}\frac{P_{l-1}(x) - P_{l+1}(x)}{l+1}\right] \quad (2)$$

where $P_{(l)}$ is the Legendre polynomial of order l.

Let us then introduce numerical values for diffusion to the active site of AChE of TFK^+, of TFK^0, and of NMA, a charged ligand characterized by essentially the same diffusion coefficient as TFK^+ and TFK^0 (Fig. 3 *A*).

A value of 32 Å for the hydrodynamic radius, R, of AChE is taken from the study of Antosiewicsz et al. (1995a). The value of ρ can be estimated by subtracting the transit region of the gorge (as defined in Methods) from the value of R, and the value of ϑ can be estimated by taking arctan (r/g), where r is the radius of the gorge mouth as defined in Methods, and g is the total gorge length. Inspection of the crystallographic 3D structure of *Tc*AChE and mAChE yields values of 8 Å for r and 24 Å for g (of which 4 Å constitute the binding region and 20 Å the transit region). These figures result in a value of ~18° for ϑ and 0.38 for s (for an active site buried ~20 Å deep in the center of a protein of 32-Å radius). If we assume that TFK^+, TFK^0, and NMA are characterized by diffusion constants similar to that of ACh, we can employ the value of $D = 61.2 \times 10^{-7}$ $cm^2\ s^{-1}$ (Antosiewicz et al., 1995a).

Introducing the values for R, ρ, ϑ, s, and D into Eq. 1 yields a value of $k = 0.21 \times 10^9\ M^{-1}\ s^{-1}$ for diffusion of these ligands to the active site of AChE buried ~60% ($\rho/R = s = 0.38$) of the way down a conical duct of aperture $\vartheta = 20°$. Values for k were calculated using the program MATLAB (Version 5.1, 1998, Mathworks, Inc.). The values tabulated in Table 2 reveal a good agreement with experimental values gathered for TFK^0; but values for the charged ligands, TFK^+ and NMA, are between 10- and 80-fold larger (depending on whether the data were collected at very high or very low ionic strength, respectively).

Our guiding assumption for explaining the faster diffusion of cationic species relative to their isosteric counterparts is that positively charged ligands and substrates will diffuse in 3D until they reach a negatively charged area at the entrance to the active-site gorge. This area will act as a perfect sink for positively charged ligands, which will undergo a reduction in dimensionality of diffusion from 3D to 1D (Adam and Delbrück, 1968) and be committed to travel to the bottom of the gorge by a negative potential gradient. Because each encounter with this trap will be productive, in effect "raising" the buried active site to the surface, it can be modeled as a spherical patch on the surface of the enzyme. In the case of neutral isosteric ligands, which should neither interact with the trapping surface nor be influenced by the gorge potential gradient, an encounter will be considered productive only if the ligand hits the spherical cap at the

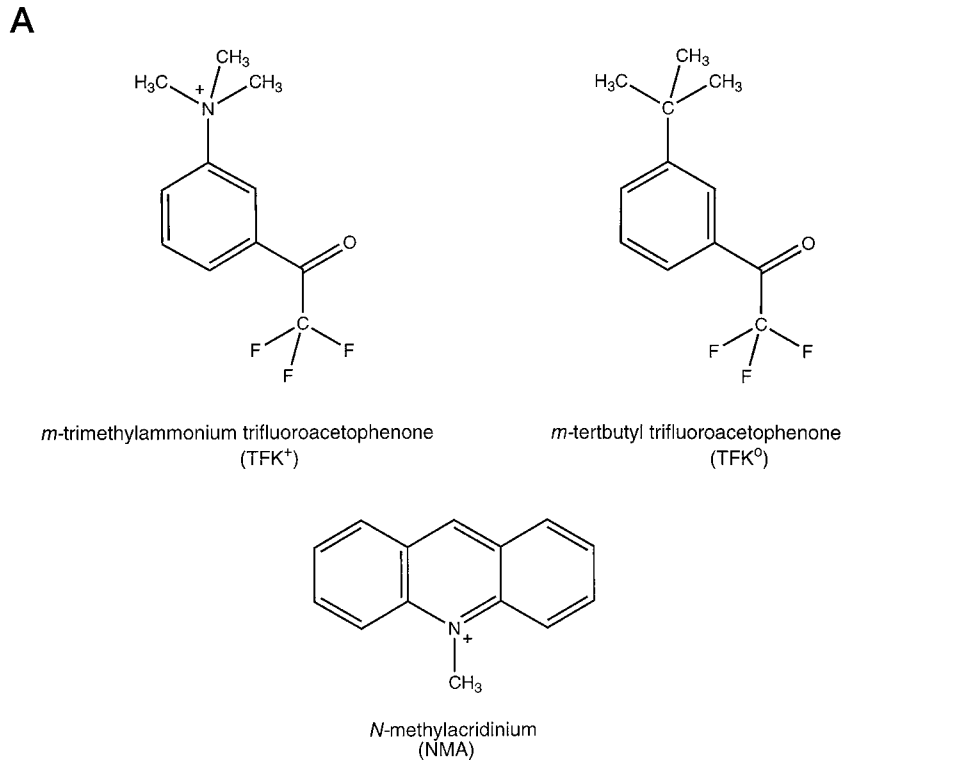

FIGURE 3 (*A*) Molecular structure of the transition-state analogs, TFK^+ and TFK^0, and of NMA. (*B*) Molecular structures of ACh, BCh, and some neutral substrates of the ChEs.

bottom of the gorge. Thus, even though the gorge may restrict the mobility of neutral species, they can effectively be considered to be searching for the buried active site as if diffusion were taking place in 3D, because their diffusion is not facilitated by a surface trap or by the negative potential gradient.

If we then assume a surface trap around the gorge area of a ChE molecule for cationic ligands, $s = 1$, and the model gives the following expression for the rate constant:

$$k(\vartheta) = 4\pi DR\frac{1}{2}[1 - \cos\vartheta]/\eta(\cos\vartheta) \qquad (3)$$

Introducing the appropriate numerical values, we get $1.5 \times 10^9\ M^{-1}\ s^{-1}$ as the limit of diffusion for TFK^+ (or

TABLE 2 Experimental inhibition constants and on rates of TFK^+, TFK^0, and NMA and comparison with theoretical values

Enzyme	K_i^0 (10^{-12} M^{-1})	K_i^H (10^{-12} M^{-1})	k_{on}^0 (10^9 M^{-1} s^{-1})	k_{on}^H (10^9 M^{-1} s^{-1})	$k_{on}^{H\ theor}$ (10^9 M^{-1} s^{-1})
TFK^+					
WT *Tc*AChE[#]	0.002 (I = 5 mM)	0.033 (I = 600 mM)	80 (I = 5 mM)	3.9 (I = 600 mM) 6.0 (I = 125 mM)	1.5
WT mAChE[§]	0.001 (I = 0 mM)	0.01 (I = 670 mM)	16 (I = 0 mM)	2.1 (I = 670 mM)	1.5
(D74N) mAChE[§]	0.14 (I = 0 mM)	1.0 (I = 670 mM)	0.65 (I = 0 mM)	0.10 (I = 670 mM)	0.21*
NMA					
WT *Ee*AChE[¶]	1200 (I = 1 mM)	26000 (I = 125 mM)	6.3 (I = 1 mM)	0.80 (I = 125 mM)	1.5
TFK^0					
WT *Tc*AChE[#]	—	3.6 (I = 250 mM)	—	0.30 (I = 250 mM)	0.21
WT *Ee*AChE[‖]	—	1.9 (I = 250 mM)	—	0.12 (I = 250 mM)	0.21
WT mAChE[§]	6.8 (I = 0 mM)	3.1 (I = 670 mM)	0.05 (I = 0 mM)	0.08 (I = 670 mM)	0.21
(D74N) mAChE[§]	5.6 (I = 0 mM)	5.6 (I = 670 mM)	0.07 (I = 0 mM)	0.10 (I = 670 mM)	0.21

The superscripts ^{0} and ^{H} refer, respectively, to measurements performed at low and high salt concentrations. The superscript ^{theor} refers to theoretical values.
*Because neutralization of the charge on residue D72 results in abolition of the surface trap, the theoretical value is assumed to be one derived from Eq. (3).
[#]Quinn et al. (1995).
[§]Radic et al. (1997).
[¶]Nolte et al. (1980).
[‖]Nair et al. (1995).

NMA) toward a molecule of AChE characterized by a surface trap with $\vartheta = 20°$. As can be seen by comparing this result with the values in Table 2, agreement with experimental data is very good for on rates measured at high ionic strength. The additional acceleration of diffusion that is observed at very low ionic strengths is best explained by a steering mechanism produced by long-range electrostatic interactions arising from the global asymmetrical distribution of surface charges in ChEs (Ripoll et al., 1993; Antosiewicz et al., 1996; Felder et al., 1997).

On the basis of these observations, we can conclude that there are two separate limits for the diffusion toward ChEs of neutral and charged isosteric ligands. In the absence of a steering mechanism generated by long-range electrostatic interactions (as is the case when on rates for ligands are measured at high salt concentration), cationic substrates are characterized by a diffusion limit about one order of magnitude larger than that for neutral isosters, and this effect is achieved by means of a trapping surface at the entrance to the gorge. As can be seen from the data in Table 2, at physiological salt concentration steering effects contribute only a 1.5–2-fold acceleration. Significant steering is present only at very low salt concentrations, when long-range contributions are strongest. Even then, the steering effect is responsible for an additional increase in encounter rates for cationic ligands of only one order of magnitude, which is much lower than the 240-fold enhancement calculated on the basis of BD simulations (Zhou et al., 1996).

We can extend this treatment to the diffusion of cationic and neutral isosteric substrates (Fig. 3 *B*). At high salt concentration, in the absence of any steering effect, the k_{cat}/K_M values for ACh and BCh are 10–15-fold larger than those for the neutral substrates, DBA, phenyl acetate (PhAC), and *o*-NPB (Tables 3 and 4, column 6), and both are about one order of magnitude smaller than the respective upper diffusion limits for cationic and neutral ligands. If we take the values of k_{cat}/K_M as reflecting the catalytic efficiency of ChEs toward these two classes of substrates, we can say that the hydrolysis of both cationic and neutral substrates approaches their specific limits of diffusion.

These findings lead us to conclude that ChEs are as efficient in catalyzing the hydrolysis of neutral substrates as they are in catalyzing the hydrolysis of their isosteric cationic counterparts. The emergence of specificity for cationic substrates thus seems to arise via a mechanism geared to speed up the diffusion of positively charged substrates toward an already optimally efficient catalytic active site. This enhancement of diffusion is accomplished primarily via a surface trap whose effectiveness is independent of salt concentration, and secondarily through a salt-dependent steering effect. The manner in which they operate will be the subject of the following sections.

Module I: a surface trap for cationic species operating via short-range local interactions

Experimental evidence for the presence of a trapping surface on ChEs and for a reduction in the dimensionality of diffusion for charged reactive species comes also from a study of the influence of viscosity on the catalytic efficiency of *Ee*AChE (Hasinoff, 1982), in which the dependence of k_{cat}/K_M on $\eta^{2/3}$ was interpreted as evidence for a reaction governed by nonspecific binding of ACh to the enzyme, followed by surface diffusion to the active site. A measure of the radius of the trapping surface can be calculated by introducing the value for the on rate of a ligand into the following equation (Hasinoff, 1982):

$$k_{on} = 4\pi NDR_{eff}/1000 \quad (4)$$

where R_{eff} is the effective trap radius, N is Avogadro's number, and D is the diffusion coefficient of the ligand.

If we introduce into Eq. 4 the value for the diffusion coefficient of TFK^+ or NMA, and the on rates measured for

TABLE 3 Experimental kinetic constants for cationic substrates at high and low salt concentrations

Enzyme	K_M^0 (10^{-6} M^{-1})	K_M^H (10^{-6} M^{-1})	k_{cat}^0 (10^5 s^{-1})	k_{cat}^H (10^5 s^{-1})	k_{cat}/K_M^0 (10^8 M^{-1} s^{-1})	k_{cat}/K_M^H (10^8 M^{-1} s^{-1})
ACh						
WT *Ee*AChE*	—	—	—	—	—	0.11 ± 0.2 (glycerol)
WT *Ee*AChE*	—	—	—	—	—	0.17 ± 0.5 (sucrose)
WT *Tc*AChE#	23 (I = 1 mM)	121 (I = 500 mM)	0.20 (I = 1 mM)	0.58 (I = 500 mM)	0.98 (I = 1 mM)	0.48 (I = 500 mM)
WT hAChE§	80 ± 10 (I = 5 mM)	120 ± 20 (I = 125 mM)	0.76 ± 0.11 (I = 5 mM)	0.83 ± 0.12 (I = 125 mM)	0.87 ± 0.12 (I = 5 mM)	0.48 ± 0.08 (I = 125 mM)
WT mAChE¶	—	—	—	—	4.1 ± 0.4 (2 mM)	0.25 ± 0.03 (I = 670 mM)
(D74N) hAChE§	—	500 ± 200 (I = 145 mM)	—	0.04 ± 0.02 (I = 145 mM)	—	0.07 ± 0.02 (I = 145 mM)
(D74G) hAChE§	—	630 ± 200 (I = 145 mM)	—	0.06 ± 0.02 (I = 145 mM)	—	0.09 ± 0.02 (I = 145 mM)
(D74N) mAChE¶	—	1300 (I = 145 mM)	—	0.01 ± 0.002 (I = 145 mM)	—	0.01 (I = 145 mM)
BCh						
WT hBChE‖	—	18 (I = 145 mM)	—	0.04 ± 0.01 (I = 145 mM)	—	0.22 (I = 145 mM)
(D70G) hBChE‖	—	150 (I = 145 mM)	—	0.04 ± 0.01 (I = 145 mM)	—	0.02 (I = 145 mM)

The superscripts ^{0} and ^{H} refer, respectively, to measurements performed at low and high salt concentrations.
*Bazelyansky et al. (1986).
#Berman and Nowak (1992).
§Shafferman et al. (1992).
¶Radic et al. (1997).
‖Masson et al. (1997).

TABLE 4 Experimental kinetic constants for neutral substrates at high and low salt concentrations

Enzyme	K_M^0 (10^{-6} M^{-1})	K_M^H (10^{-6} M^{-1})	k_{cat}^0 (10^5 s^{-1})	k_{cat}^H (10^5 s^{-1})	k_{cat}/K_M^0 (10^8 M^{-1} s^{-1})	k_{cat}/K_M^H (10^8 M^{-1} s^{-1})
DBA						
WT *Ee*AChE*	—	—	—	—	—	0.01 (glycerol)
WT *Ee*AChE*	—	—	—	—	—	0.01 (sucrose)
WT *Ee*AChE#	—	260 ± 30 (200 mM)	—	0.31 (I = 200 mM)	—	0.01 (I = 200 mM)
WT *Tc*AChE§	—	—	—	0.19 (I = 250 mM)	—	0.07 (I = 250 mM)
WT hAChE¶	280 ± 40 (I = 5 mM)	260 ± 30 (I = 125 mM)	0.76 ± 0.11 (I = 5 mM)	0.83 ± 0.12 (I = 125 mM)	0.02 (I = 5 mM)	0.02 (I = 125 mM)
o-NPB						
WT hBChE‖	—	125 ± 20 (I = 145 mM)	—	0.06 ± 0.005 (I = 145 mM)	—	0.05 (I = 145 mM)
(D70G) hBChE‖	—	12 ± 20 (I = 145 mM)	—	0.06 ± 0.02 (I = 145 mM)	—	0.05 (I = 145 mM)

The superscripts ^{0} and ^{H} refer, respectively, to measurements performed at low and high salt concentrations.
*Bazelyansky et al. (1986).
#Hasan et al. (1981).
§Nair et al. (1995).
¶Shafferman et al. (1992).
‖Masson et al. (1997).

these ligands and AChE from various species at high salt concentration, we get an average value for the trap radius of ~7.5 Å, which is similar both to the mean radius of ~9 Å estimated in recent MD studies (Wlodek et al., 1997b) and to our own estimate of ~8 Å derived from the crystallographically determined structure of *Tc*AChE (Sussman et al., 1991).

Recent studies have suggested that a particular residue, D72 (D74 in mAChE and hAChE, D70 in hBChE), might contribute to the specificity of ChEs for cationic ligands by a trapping mechanism (Hosea et al., 1996; Masson et al., 1996, 1997). This residue is strategically placed near the top of the active-site gorge (Fig. 1) and was identified as a crucial component of the PAS (Shafferman et al., 1992; Barak et al., 1995). Strong evidence in support of our model comes from the observation that in mutant enzymes in which the putative cationic trap has been removed by neutralizing the charge on D72, on-rate values for cationic ligands fall to the theoretical values for neutral ones (Table 2). In addition, at physiological salt concentration, k_{cat}/K_M values for cationic substrates closely approach the values for neutral substrates when the negative charge on the side chain of residue D72 is neutralized (Table 3, column 6). These findings point to D72 as the major component of a cation-specific trap at the entrance to the active-site gorge of ChEs. Previous calculations comparing the D72N mutant to WT AChE revealed a small contribution of the negative charge of the side chain of D72 to the overall potential gradient within the active-site gorge (Felder et al., 1997). This small contribution does not correlate with the drastic reductions in both catalytic efficiency and in on rates for cationic ligands produced by mutations in this position. BD simulations of the on rates of cationic ligands have been found to be in good agreement with experimental data, but their predictions were significantly less accurate when residue D72 was neutralized (Radic et al., 1997). However, we find a good correlation between on rates for TFK^+ and the average potential in the gorge region corresponding to the cationic trap, both for WT AChE and for a series of mutants in which the charge on D72 was neutralized along with the charges on a number of surface residues, particularly D82 and D278 (Radic et al., 1997) (Fig. 4 *A*). Moreover, we also find a good correlation between on rates for TFK^+ and overall gorge potentials for surface mutants and for the E199Q mutant, whose side chain is shown to contribute significantly to the overall gorge potential (Felder et al., 1997; Wlodek et al., 1997a) (Fig. 4 *B*). These findings provide supporting evidence for our treatment of the acceleration of diffusion of cationic species as being composed of the additive effects of a surface trap operating through local short-range interactions, constituted by the side chains of a few key residues, primarily D72, D82, and D278, and of a long-range steering effect generated by the overall gorge potential.

If we want to uncouple the effects of local short-range interactions from the effect produced by long-range interactions on diffusion rates, we must resort to systems in which the mechanism necessary for the recognition of positively charged substrates is maintained, while the contribution of the negative charge on D72 to the gorge potential has been eliminated. It so happens that in all insect species studied so far, the amino acid at the position equivalent to residue 72 in *Tc*AChE is a tyrosine (Toutant, 1989; Anthony et al., 1995; Zhu and Clark, 1995). Site-directed mutagenesis studies on *Dm*AChE in which Y109 (equivalent to D72 in *Tc*AChE) was mutated to a glycine or a lysine showed that such a mutation increased the K_M for ACh by 10- and 100-fold, respectively, whereas mutation to glutamate had no effect on K_M (Mutero et al., 1992). We interpret these results as evidence for a trapping mechanism for cationic substrates and ligands mediated, in insect ChEs, by the aromatic side chain of Y109 via local cation-π interactions. The predictions made by our model are supported by a comparison of the 3D structure of *Dm*AChE, recently solved in our laboratory (Harel et al., 1999) and that of *Tc*AChE, which shows the position of residue Y109 to be almost identical to that of D72. We thus predict that the D72Y mutant in *Torpedo* or other vertebrate ChEs should retain most of its catalytic efficiency, and that any reduction in catalytic efficiency resulting from the D72Y mutation should be correlated with the corresponding small decrease in gorge potential. Our assumption that an aromatic residue can be as efficient as a negatively charged one in the recognition of cations is corroborated by the following data:

1. Cation-π interactions are predominantly electrostatic, involving the interaction of the cation with the large, permanent quadrupole moment of the aromatic ring (Dougherty, 1996).
2. Gas-phase measurements of binding energy of cations to benzene and to toluene have shown that in this phase a cation would preferentially bind to an aromatic compound rather than to water (Sunner et al., 1981).
3. In an aqueous environment, a pocket lined with the side chains of amino acids such as Trp, Phe, and Tyr can efficiently compete with full water solvation for the stabilization of a positive charge, because of the sizable quadrupole moment of the rings of aromatic residues (Luhmer et al., 1994). The importance of cation-π interactions in the catalytic function of ChEs has been confirmed by a large body of structural (Sussman et al., 1991; Harel et al., 1993, 1996) and kinetic (Ordentlich et al., 1993; Radic et al., 1993; Nair et al., 1994; Barak et al., 1995) data.

Modeling of the D72Y mutant of *Tc*AChE shows that the hydroxyl moiety of the tyrosine at position 72 is capable of forming a hydrogen bond with Y121. It has been hypothesized that the hydrogen bond between Y121 and D72 in WT AChE is required for maintaining the "functional crosstalk" postulated for the transduction of allosteric signals from the PAS to the catalytic center (Shafferman et al., 1992; Barak et al., 1995). These considerations also provide us with a rather straightforward test for the presence of such

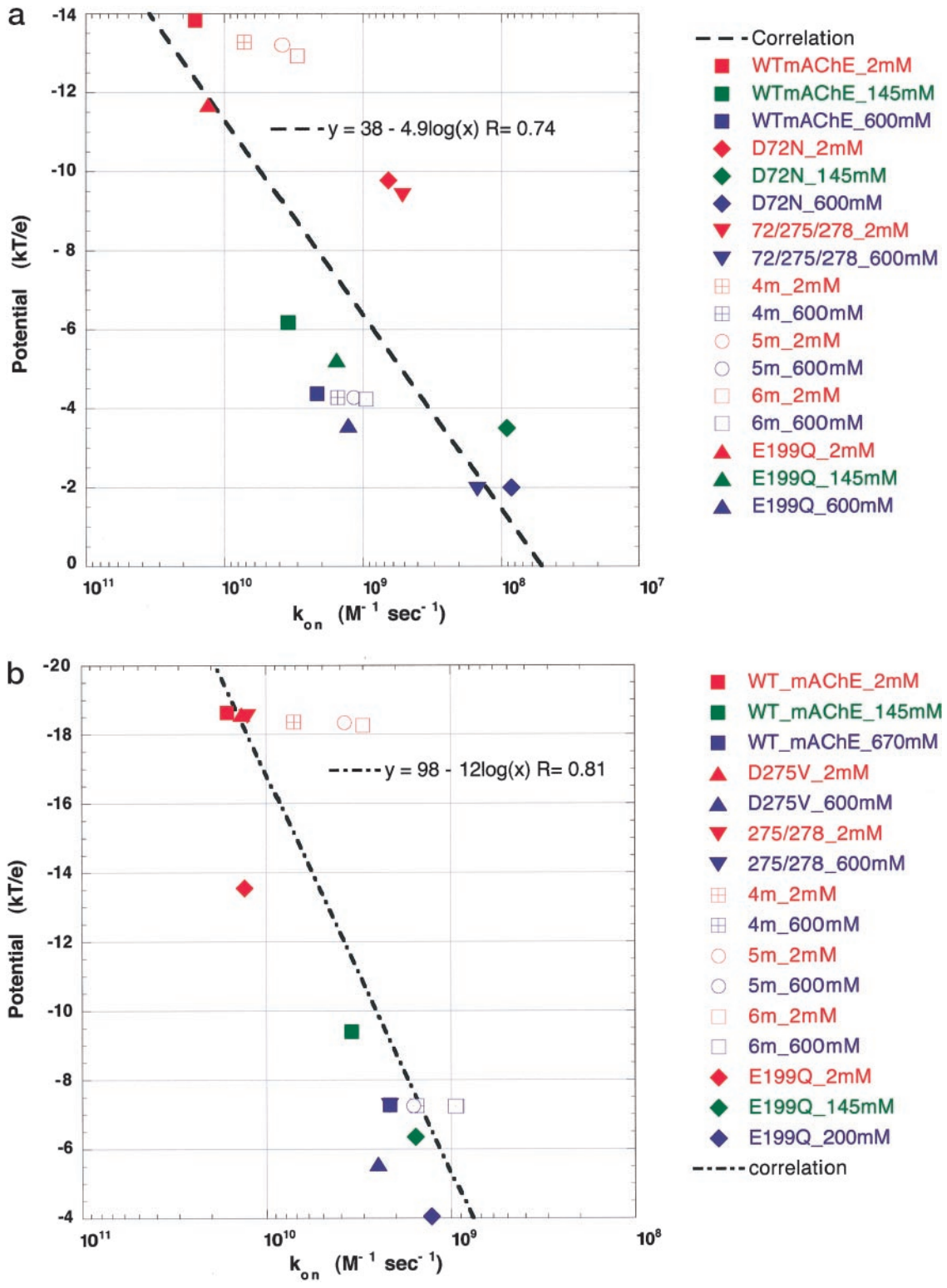

FIGURE 4 (*A*) Correlation between average potentials in the trap region and encounter rates for TFK^+ at high (600 mM), physiological (145 mM), and low (2 mM) salt concentrations. The potential values are calculated for WT mAChE and for the following mutants (the abbreviations used in the list on the right of the figure are given in parentheses): D72N (D72N); D72N/D275V/D278N (72/275/278); E82Q/E89Q/D275V/D278N (4m); E82Q/E89Q/D275V/D278N/D365N (5m); E82Q/E89Q/D275V/D278N/E285Q/D365N (6m). (*B*) Correlation between overall gorge potential and encounter rates for TFK^+ at high (600 mM), physiological (145 mM), and low (2 mM) salt concentrations. The potential values are calculated for WT mAChE and for the following mutants (the abbreviations used in the list on the right of the figure are given in parentheses): D275V (D275V); D275V/D278N (275/278); E82Q/E89Q/D275V/D278N (4m); E82Q/E89Q/D275V/D278N/D365N (5m); E82Q/E89Q/D275V/D278N/E285Q/D365N (6m); E199Q (E199Q).

cross-talk, because replacing tyrosine with phenylalanine, i.e., generating the D72F mutant, should have a disruptive effect on signal transduction and reduce catalytic efficiency significantly. Analysis of the kinetic properties of these mutants is under way, and preliminary results show that the K_M values of both D72Y and D72F mutants of *Tc*AChE are not significantly different from those of WT-*Tc*AChE, thus providing strong supportive evidence for our hypothesis. A complete analysis of the catalytic properties of these mutants, along with other mutants generated to study the role of aromatic and charged residues inside the active-site gorge of ChEs, is currently under way (S. A. Botti, E. Krejci, S. Bon, D. M. Quinn, J. L. Sussman, I. Silman, and J. Massoulié, manuscript in preparation).

Module II: the potential gradient along the active-site gorge is responsible for steering cationic species to the active site of ChE

We now turn our attention to the second module of our treatment: the long-range electrostatic steering effect. We will discuss how this effect arises from the potential gradient along the gorge axis, which arises from the combined effect of the overall charge distribution in the ChE molecule and the contribution of several α-helix dipoles. Kinetic studies have revealed both a marked reduction in the affinity of AChE for cationic substrates and inhibitors (Mendel and Rudney, 1943) and an increase in k_{cat} (Nolte et al., 1980; Smissaert, 1981; Hofer et al., 1984), upon the addition of inorganic salts such as sodium or magnesium chloride. The dependence upon salt concentration has been ascribed to the binding of inorganic cations to anionic sites (Taylor and Lappi, 1975; Smissaert, 1981), to conformational changes resulting from occupation of the PAS by metal ions (Changeux, 1966), and to the screening of favorable electrostatic interactions between the cationic substrate and the "anionic" subsite in the active site of the enzyme (Dawson and Crone, 1973; Nolte et al., 1980; Hofer et al., 1984). Comparison of the effects of monovalent and divalent ions on the activity of AChE suggests a general screening effect of monovalent cations, while it has been proposed that divalent cations interact specifically with carboxylate groups present in the active site (Hofer et al., 1984). The identification of a putative binding site for Zn^{2+} in hBChE (Bhanumathy and Balasubramanian, 1996) supports the notion of specific binding sites for divalent cations in ChEs.

The potential gradient along the gorge axis and its dependence on salt concentration have been calculated both for WT *Tc*AChE and for a series of surface and active-site mutant models (Antosiewicz et al., 1995b; Felder et al., 1997; Wlodek et al., 1997a). On the basis of these results, it has been suggested that enhancement of encounter rates between cationic ligands and the catalytic machinery buried near the bottom of the active-site gorge is due to long-range electrostatic interactions, attributable to the potential drop along the length of the active-site gorge. Radic et al. (1997) recently analyzed in detail the influence of electrostatics on the kinetics of ligand binding to AChE. Their study focused on the ionic-strength dependence of the binding of ligands to AChE after neutralization, through site-directed mutagenesis, of the negative charges of residues in the active site, in the PAS, and within a surface area around the entrance to the gorge. Comparison of experimental on rates for TFK^+ gathered on the surface and active-site mutants revealed good agreement with BD simulations. However, prediction of on rates after neutralization of the negative charge of D72, which is considered to be a major component of the PAS, was considerably less accurate. Radic et al. (1997) interpreted their results by assuming two distinct types of electrostatic interaction: one interaction, dependent on salt concentration, brings about acceleration of the initial encounter rates of cationic ligands with the enzyme, and a second one, independent of salt concentration, results in trapping of these ligands by specific residues within the PAS.

Fig. 5 shows that the ionic-strength-dependent decrease in electrostatic potential inside (and outside) the active-site gorge is rather well correlated with the corresponding decrease in encounter rates of both NMA and TFK^+ with *Ee*AChE, *Tc*AChE, and mAChE (Nolte et al., 1980; Berman et al., 1991). It thus seems reasonable to argue that this correlation corresponds to the contribution to molecular traffic of salt-dependent long-range interactions arising from the global asymmetrical distribution of charges in ChEs.

This argument is reinforced by the observation that neutralization of seven negatively charged residues around the entrance to the active-site gorge has only a small effect on the potential gradient within the active-site gorge (Felder et al., 1997), and that this small change is strongly correlated with a concomitant small reduction in catalytic efficiency (Shafferman et al., 1994). The overall potential difference along the axis of the active-site gorge is similar for AChE of different species and is ~20% smaller for hBChE, as shown in Fig. 6. In this figure, it is interesting to note that the slope of the potential gradient displays an inflection ~14 Å from the bottom of the gorge, in the neighborhood of D72, D82, and D278. Antosiewicz et al. (1995b) pointed out that the profile of rate constant versus depth of penetration inside the gorge suggests a "choke point" in the same region, beyond which the reactive species becomes committed to a productive encounter. In *Dm*AChE, where the residue homologous to D72 is a tyrosine (Y109), the inflection in gorge potential is less pronounced than for vertebrate AChEs. Our hypothesis is that this smaller inflection is due to the contribution of conserved negatively charged residues in *Dm*AChE (Felder et al., 1997), homologous to D82 and D278, which constitute the secondary components of the cationic surface trap. These considerations strengthen the case for a major role of D72, and secondarily of D82 and D278, in the recognition of cationic substrates.

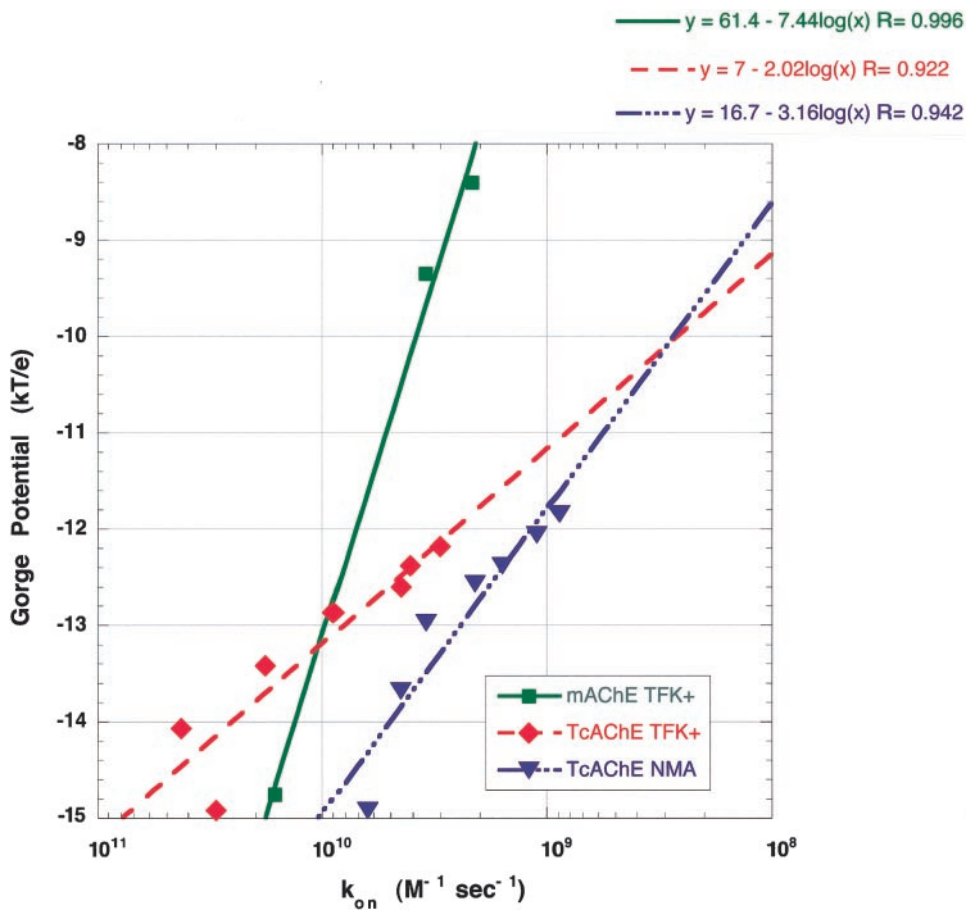

FIGURE 5 Correlation between overall gorge potentials of WT AChEs and encounter rates of TFK^+ and NMA as a function of salt concentration. The potential values were calculated for *Tc*AChE for salt concentration values varying from 2 to 600 mM.

Part II: quantitative treatment of the electrostatic forces underlying ChE-ligand binding interactions

Contribution of electrostatic interactions to the binding of transition-state analogs to ChEs

In the previous sections we showed that diffusion of cationic species toward the active site of ChEs is enhanced both by a cationic trap, which operates through local short-range electrostatic interactions, and by a steering effect that emerges from the global asymmetrical spatial distribution of charges in the ChE molecule. In this section we analyze the contribution of a single positive charge to the stabilization of the binding of transition-state analogs to ChEs, with a treatment analogous to the one used in the previous sections. Binding experiments have revealed a strong dependence upon ionic strength of the K_i of TFK^+, which is not observed for TFK^0 (Radic et al., 1997). Mutation studies have shown that stabilization of the binding of both TFK^+ and TFK^0 is primarily due to short-range interactions between W84 and the quaternary ammonium (*tert*-butyl) moiety of TFK^+ (TFK^0) (Radic et al., 1995, 1997), which take the form of cation-π interactions in the case of TFK^+ and of short-range London dispersion forces in the case of TFK^0 (Nair et al., 1994). These studies show that binding of TFK^+ to the W86A (*W84A*) mutant of mAChE is ~1500-fold weaker than binding to WT mAChE. In contrast, mutation of E199 or E443 (near the gorge floor) results in only a ~10-fold decrease in binding strength, and neutralization of the negative charge on D72 (at the top of the gorge) in only a 20-fold decrease. Moreover, only the mutation of W84 affects the binding strength of TFK^0 to AChE (Radic et al., 1995, 1997; Hosea et al., 1996). The primary role of W84 in the binding of these transition-state analogs has been confirmed by the solution of the 3D structure of the complex of TFK^+ and *Tc*AChE (Harel et al., 1996), and we can reasonably assume that the neutral analog, TFK^0, would bind in an analogous fashion.

Consequently, we can consider the overall "charge effect," i.e., the added stabilization to the binding energy of cationic transition state analogs for ChEs relative to their neutral isosteric counterparts, to be composed of two independent contributions, both electrostatic:

1. A global term arising from long-range electrostatic contributions that are screened at high salt concentrations.
2. A local term that can be identified with cation-π and local, short-range electrostatic interactions between the charged substrates and key binding residues, such as W84, in the active-site gorge.

The difference in binding between TFK^+ and TFK^0 due to the positive charge, which we shall term $\Delta\Delta G_{charge}$, can

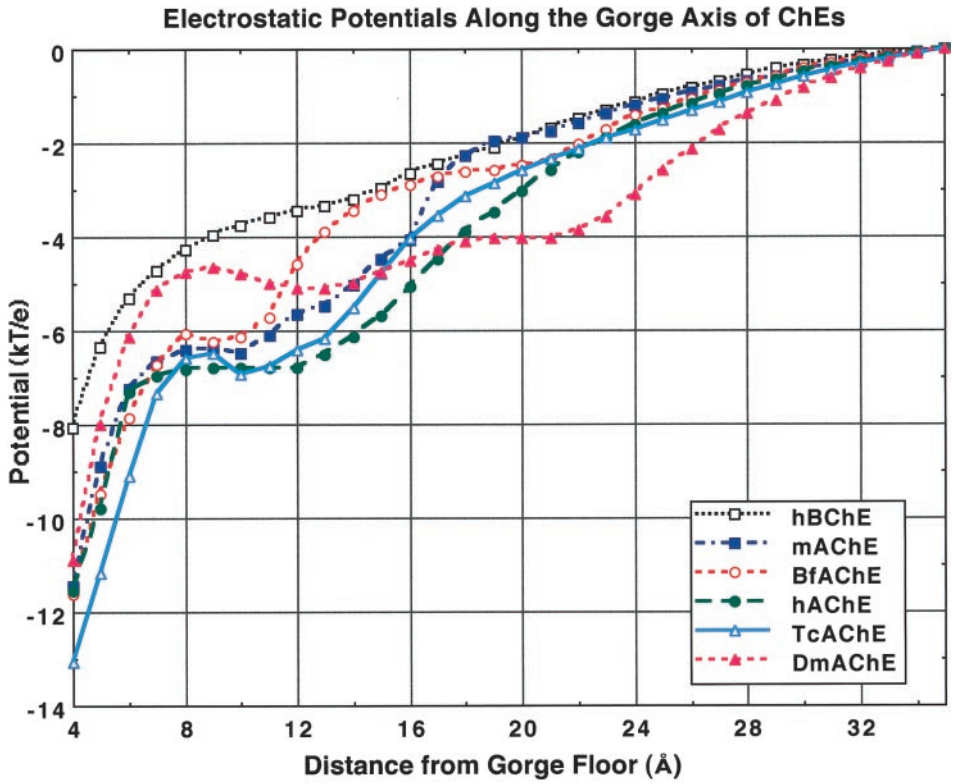

FIGURE 6 Electrostatic potentials along the gorge axis for ChEs. The potentials were calculated for *Tc*AChE, mAChE, hAChE, *Dm*AChE, *Bf*AChE, and hBChE.

be calculated from the experimentally determined dissociation constants measured for WT mAChE and can be defined as

$$\Delta\Delta G_{\text{charge}} = \Delta G_{\text{TFK}^+} - \Delta G_{\text{TFK}^0} \tag{5}$$

With $\Delta G_{\text{TFK}^+} = -RT \ln K_{\text{i TFK}^+}$ and $\Delta G_{\text{TFK}^0} = -RT \ln K_{\text{i TFK}^0}$ it follows that

$$\Delta\Delta G_{\text{charge}} = RT \ln (K_{\text{i TFK}^0}/K_{\text{i TFK}^+}) \tag{6}$$

If we assume $\Delta\Delta G_{\text{charge}}$ to be the sum of all local interactions between the quaternary ammonium (*tert*-butyl) moiety of TFK^+ (TFK^0) and the aromatic side chains in the acyl binding pocket, and of global electrostatic interactions due to the potential gradient within the active-site gorge, we can express $\Delta\Delta G_{\text{charge}}$ as

$$\Delta\Delta G_{\text{charge}} = \Delta\Delta G_{\text{L}} + \Delta\Delta G_{\text{G}} \tag{7}$$

in which

$$\Delta\Delta G_{\text{L}} = \Delta G_{\text{L TFK}^+} - \Delta G_{\text{L TFK}^0} \tag{8}$$

and

$$\Delta\Delta G_{\text{G}} = \Delta G_{\text{G TFK}^+} - \Delta G_{\text{G TFK}^0} \tag{9}$$

If we consider the major contribution to the local term to be due to interaction of TFK^+ and TFK^0 with W84, we can isolate the contribution to the global term by considering the change in K_{i} between WT AChE and the W84A. Although it is possible that the W84A mutation may produce structural rearrangements, these should affect binding of both TFK^+ and TFK^0 similarly, so that the only effect measured will be that produced by the difference in charge of the two inhibitors.

In this case,

$$\begin{aligned}\Delta\Delta G_{\text{G}} &= \Delta G_{\text{W84A TFK}^+} - \Delta G_{\text{W84A TFK}^0} \\ &= RT\ln(K_{\text{i W84A TFK}^0}/K_{\text{i W84A TFK}^+})\end{aligned} \tag{10}$$

The value of the contribution to the local term can similarly be isolated and assessed by examining the difference in binding energy between TFK^+ and TFK^0 at very high salt concentrations, where the steering effect should be completely screened. In this case,

$$\begin{aligned}\Delta\Delta G_{\text{L}} &= \Delta G_{\text{high TFK}^+} - \Delta G_{\text{high TFK}^0} \\ &= RT\ln(K_{\text{i high TFK}^+}/K_{\text{i high TFK}^0})\end{aligned} \tag{11}$$

We can safely assume the value of $K_{\text{i TFK}^0}$ to be independent of salt concentration because global electrostatic forces should have little effect on TFK^0 (Quinn et al., 1995; Radic et al., 1997).

If our assumptions are correct, the experimental data gathered for these systems should yield values for $\Delta\Delta G_{\text{L}}$ and $\Delta\Delta G_{\text{G}}$ which, when summed, should give back the experimentally measured value for $\Delta\Delta G_{\text{charge}}$.

The validity of our assumption is shown in Table 5. Substituting in Eqs. 5, 10, and 11 the appropriate experimental K_{i} values for TFK^+ and TFK^0, tabulated in column 1 of Table 5, yields values for $\Delta\Delta G_{\text{L}}$ of ~3.4 kcal/mol and for $\Delta\Delta G_{\text{G}}$ of 0.4 kcal/mol for $I = 0.145$ mM and of 1.4

TABLE 5 Experimental values of K_i for TFK^+ and TFK^0 employed in the calculation of $\Delta\Delta G_{charge}$, $\Delta\Delta G_L$, and $\Delta\Delta G_g$

Enzyme	K_i TFK^+ (10^{-12} M)	K_i TFK^0 (10^{-12} M)	$\Delta\Delta G$ (kcal M^{-1})
WT *Tc*AChE*	0.002 (I = 2 mM)	3.6 (I = 2 mM)	4.3 (total)
WT *Tc*AChE#	0.003 (I = 600 mM)	3.6 (I = 600 mM)	2.9 (local)
WT mAChE#	0.001 (I = 2 mM)	3.6 (I = 2 mM)	4.7 (total)
WT mAChE§	0.005 (I = 145 mM)	3.7 (I = 145 mM)	3.8 (total)
WT mAChE#	0.012 (I = 670 mM)	3.6 (I = 670 mM)	3.4 (local)
(W84A) mAChE§	7.7	78	1.4–0.4 (global)

*Quinn et al. (1995).
#Radic et al. (1997).
§Radic et al. (1995).

kcal/mol for $I = 0.02$ mM. Substitution of these values in Eq. 7 yields values for $\Delta\Delta G_{charge}$ of 3.8 kcal/mol and 4.8 kcal/mol, at physiological and low salt concentrations, respectively, thus supporting our hypothesis.

Calculation of the potential inside the active-site gorge of AChE from $\Delta\Delta G^{\ddagger}$ values for the activated complex of AChE with TFK^+ and TFK^0

Having established that measurement of the difference in K_i between TFK^+ and TFK^0 provides a powerful tool for calculating the contributions of electrostatic interactions, one can ask if the same tool can be employed to measure the electrostatic potential within the active site, and if values so obtained will be in agreement with the ones calculated by solving the PB equation for the system in question.

In a recent study (Stauffer and Karlin, 1994), the electrostatic potential of ACh binding sites in the nicotinic ACh receptor (nAChR) was measured by analyzing the rate constants for the reactions of charged and neutral methanethiosulfonates with binding-site cysteines within the nAChR in terms of absolute rate theory and Debye-Huckel theory, which, together, can be used to obtain rate constants as a function of the electrostatic potential, the charges of the reactants, and the ionic strength of the solution (Laidler, 1965).

This treatment was applied to our system in an analogous fashion. TFK^+ and TFK^0 bind to ChEs by forming a hemiketal adduct with the active-site serine, S200. Reaction of either TFK^+ or TFK^0 with AChE (Quinn et al., 1995) can be considered to take place according to the following scheme:

$$E + I \underset{k_{off}}{\overset{k_{on}}{\rightleftharpoons}} EI$$

Formation of the hemiketal adduct can be considered as proceeding through a short-lived activated complex, $EI^{\ddagger}$. Transition state theory provides the relationship between rate constants and free energies of the enzyme, the inhibitor, their complex, and the activated binding state (Glasstone et al., 1941):

$$k_{on\ TFK} = \nu \exp(-\Delta G^{\ddagger}_{on}/RT) \tag{12.1}$$

$$k_{off\ TFK} = \nu \exp(-\Delta G^{\ddagger}_{off}/RT) \tag{12.2}$$

where ν is the vibrational frequency of the activated complex in the degree of freedom leading to its decomposition, and

$$\Delta G^{\ddagger}_{on} = G^0_{EI^{\ddagger}} - G^0_E + G^0_I \tag{13.1}$$

$$\Delta G^{\ddagger}_{off} = G^0_{EI^{\ddagger}} - G^0_{EI} \tag{13.2}$$

We can then apply the reasoning used in the previous section to determine the contribution of global and local terms to $\Delta\Delta G_{charge}$, and consider the global contribution of long-range interactions separately from all other contributions, including nonelectrostatic interactions, which we will bundle into the local term. In this case,

$$\Delta G^{\ddagger}_{on} = \Delta G^{\ddagger}_{onL} + \Delta G^{\ddagger}_{onG} \tag{14}$$

The change in electrostatic energy due to the global term can be expressed as the sum of the energies associated with uncharging of the ionic atmospheres of the reactants, and with charging of the ionic atmosphere of the activated binding complex, so that

$$\Delta G^{\ddagger}_{onG} = z_{TFK} F \psi_E + RT \ln(\gamma_{EI^{\ddagger}}/(\gamma_E\ \gamma_I)) \tag{15}$$

where ψ_E, expressed in volts, is the electrostatic potential due to E at the reaction radius at zero ionic strength; z_{TFK} is the charge of TFK; γ_E, γ_I, and $\gamma_{EI^{\ddagger}}$ are, respectively, the molar activity coefficients of enzyme, inhibitor, and activated complex; and F is the Faraday constant. The first term on the right is the electrostatic free energy for formation of the activated complex in the absence of ionic atmospheres, and the second term on the right is the difference in the free energies of charging of the ionic atmospheres of the complex and of the reactants.

Combining Eqs. 12, 14, and 15, we obtain, for TFK^+,

$$\ln(k_{on\ TFK^+}) = \ln(k_L) - F/RT(z_{TFK^+}\psi_E + \ln(\gamma_{EI^{\ddagger}}/\gamma_E\gamma_I)) \tag{16}$$

where $k_{on\ TFK^+} = \nu \exp(\Delta G^{\ddagger}_{onL}/RT)$.

If we take the ratios between the on rates of TFK^+ and TFK^0, we get the following expression:

$$\ln(k_{on\ TFK^+}/k_{on\ TFK^0}) = \ln(k_{L\ TFK^+}/k_{L\ TFK^0}) - F/RT(z_{TFK^+}\psi_E + \ln(\gamma_{EI^{\ddagger}}/\gamma_E\ \gamma_I)) \tag{17}$$

or

$$RT\ln(k_{\text{on TFK}^+}/k_{\text{on TFK}^0}) = -\Delta\Delta G^{\ddagger}_{\text{on L}} - F(z_{\text{TFK}^+}\psi_{\text{E}} + \ln(\gamma_{+EI^{\ddagger}}/\gamma_{\text{E}}\,\gamma_{\text{I}})) \quad (18)$$

where the long-range term will be contributed only by TFK^+, because TFK^0 binding is not dependent on long-range electrostatic interactions.

Using an approach analogous to that used to calculate $\Delta\Delta G_{\text{L}}$ in the previous section, we can calculate $\Delta\Delta G^{\ddagger}_{\text{onL}}$ from the ratio of on rates for TFK^+ and TFK^0 at very high salt concentrations, where, as may be recalled, the global interactions should be completely screened and the long-range term for TFK^+ can be considered negligibly small:

$$\Delta\Delta G^{\ddagger}_{\text{onL}} = -RT\ln(k_{\text{on high TFK}^+}/k_{\text{on high TFK}^0}) \quad (19)$$

Substituting Eq. 19 into Eq. 18, we get the following expression:

$$RT\ln(k_{\text{on TFK}^+}/k_{\text{on TFK}^0}) = RT\ln(k_{\text{on high TFK}^+}/k_{\text{on high TFK}^0}) - F(z_{\text{TFK}^+}\psi_{\text{E}} + \ln(\gamma_{\text{EI}^{\ddagger}}/\gamma_{\text{E}}\,\gamma_{\text{I}})) \quad (20)$$

The dependence of the rate constant of TFK^+ on the electric potential is free of geometric assumptions. Its dependence on ionic strength, however, is derived with a number of simplifying assumptions, including spherically symmetrical ions. Subject to these assumptions, and at the limit of low ionic strength, we can express

$$\log(\gamma) = -Qz^2I^{1/2} \quad (21)$$

where $Q = 1.826 \times 10^6/(\varepsilon T)^{3/2}$, ε is the dielectric constant, and I is the ionic strength. At 25°C in water ($\varepsilon = 80$), $Q = 0.51\ \text{M}^{-1/2}$; thus combining Eqs. 20 and 21 and dividing by RT, we get

$$\log(k_{\text{on TFK}^+}/k_{\text{on TFK}^0}) = RT\log(k_{\text{on high TFK}^+}/k_{\text{on high TFK}^0}) - 0.434F/RT(z_{\text{TFK}}\psi_{\text{E}} + z_{\text{TFK}}z_{\text{E}}I^{1/2}) \quad (22)$$

for very low ionic strength the term $z_{\text{TFK}^+}z_{\text{E}}I^{1/2}$ becomes negligible, and we get (at 298.13K, 0.434 F/RT 17)

$$\log(k^0_{\text{on TFK}^+}/k^0_{\text{on TFK}^0}) = \log(k_{\text{on high TFK}^+}/k_{\text{on high TFK}^0}) - 17z_{\text{TFK}^+}\psi_{\text{E}} \quad (23)$$

which expresses the ratio of the on rates for TFK^+ and TFK^0 at very low ionic strength as a function of the electrostatic potential in the gorge of AChE. As can be calculated by taking the appropriate values from column 4 of Table 2, the electrostatic potentials inside the gorges of *Tc*AChE and mAChE are −80.4 mV and −71.2 mV, respectively. These values constitute the upper limit of the overall gorge potential at zero ionic strength and give a value for $\Delta\Delta G^{\ddagger}_{\text{onG}}$ of ~1.6 kcal/mol, which can be considered to be the maximum contribution of global electrostatic interactions to the stabilization of the activated binding state.

Potential values obtained by solving the PB equation exceed the ones calculated from the above experimental data by approximately fourfold (Felder et al., 1997; Wlodek et al., 1997b). While both methods involve several approximations, we are inclined to think that the methods using the PB equation might overestimate the potential inside the active-site gorge due to the inherent error involved in calculating the field within very tight crevices such as the active-site gorge, where the environment can be considered neither fully solvated nor completely devoid of water molecules.

Part III: product clearance from the active-site gorge

The electrostatic potential gradient inside the active-site gorge of ChEs does not retard clearance of positively charged products

One of the open questions concerning the mechanism of molecular traffic through the active-site gorge of ChEs is whether the effect of the electrostatic potential on the positively charged product of catalysis, choline (Ch), might be so strong as to impede its exit and, if so, whether there might be an alternative route for product traffic. The clearance of the other products of ACh hydrolysis has not attracted as much attention as that of their positively charged partner. In the case of acetate and acetic acid, the anionic and neutral nature of these molecules argues against an electrostatic impediment to clearance through the gorge. In the case of the proton, its clearance probably occurs either via water molecules present in the gorge or via coupling to the acetate ion (D. van Belle and S. Wodak, personal communication), and no hindrance from the gorge potential to its release has been suggested.

To establish whether the magnitude of the electrostatic potential inside the gorge is sufficient to sensibly retard the clearance of cationic species from the active site, we chose to describe this process by treating the exit of Ch from the gorge as a 1D escape from a well in the presence of a linear potential (Fig. 7). Accordingly, Ch will be modeled as a spherical particle with a single positive charge, and interactions with the walls of the gorge will be ignored. The gorge will be considered as a one-dimensional box, 20 Å long, filled with water (Fig. 7). The effect of an electrostatic potential gradient on the rate of migration of a cationic ligand can be modeled by calculating the mean escape time $\langle t\rangle$ of a particle in a 1D potential well. The value of $\langle t\rangle$ can be derived as (Lifson and Jackson, 1962)

$$\nabla\cdot(e^{\phi}\nabla\langle t\rangle) = -e^{\phi}/D \quad (24)$$

where D is the diffusion constant of the ligand, and $\phi = -\psi(e/kT)$ is a reduced dimensionless electrostatic potential, where ψ is expressed in units of kT/e. Although not strictly correct, we can assume for the present purpose the potential

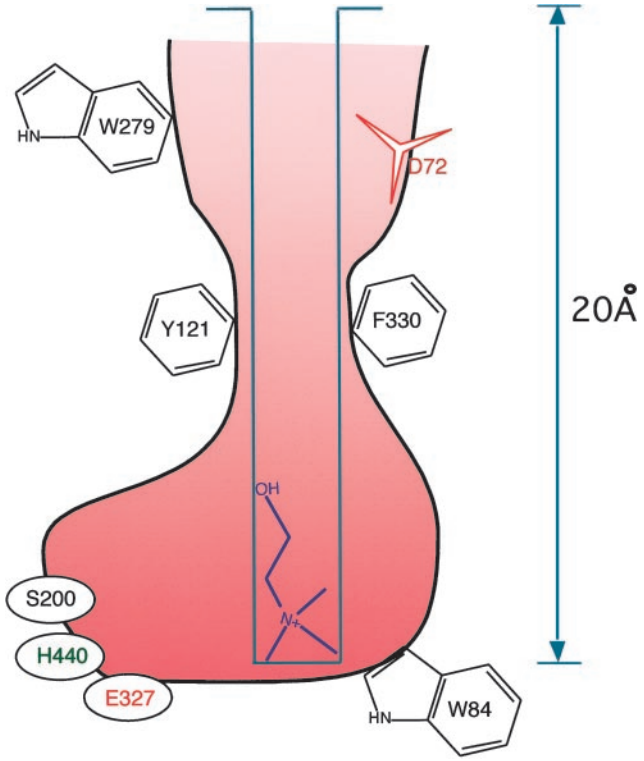

FIGURE 7 Schematic of the active-site gorge of AChE and model for the escape of choline from a one-dimensional potential well. The potential well is delimited by the green lines, and the bottleneck formed by F300 and Y121 is indicated by the benzene rings midway up the gorge.

gradient inside the gorge to be linear in distance. Accordingly, if L is the length of the gorge, the solution to Eq. (23) is

$$\langle t\rangle = (e^{\phi L} - 1 - \phi L)/D\phi^2 \tag{25}$$

In the special case of $\phi = 0$, and assuming a value of the diffusion constant, D, for Ch equal to that of ACh (6.1×10^{-6} cm^2 s^{-1}), we get

$$\langle t\rangle = L^2/2D = (2.0 \times 10^{-7}\ \text{cm})^2/2 \cdot (6.1 \times 10^{-6}\ \text{cm}^2\ \text{s}^{-1}) = 3.3 \times 10^{-9}\text{s} \tag{26}$$

In the case of the value that we calculated for the potential ψ at the bottom of the active-site gorge of 80 mV (which is $\sim 3kT/e$), Eq. 24 yields the following escape time:

$$\langle t\rangle = (L^2/2D)(2e^{\phi}/\phi^2) = (3.3 \times 10^{-9}\ \text{s}) \times 2\exp(3)/3^2 = 1.5 \times 10^{-8}\ \text{s} \tag{27}$$

This is ~4.5-fold slower than the calculated escape time in the absence of the field. If it is assumed that varying the field does not affect any chemical step in the enzymatic hydrolysis, we can check the validity of our assumption by inspecting the variation of k_{cat} for ACh with salt concentration. It can be seen that at very low salt concentration, where the steering effect should be felt most strongly, turnover is just ~5 times slower than at $I = 600$ mM, when the effect of the field should be completely screened by salt effects (Table 6). Because the strength of the field inside the active site gorge drops logarithmically with increasing ionic strength, its influence at physiological salt concentrations will be even less significant. From this result it can be seen that the presence of an electrostatic steering mechanism does not greatly influence the clearance of products from the gorge.

We are aware that the model we are employing is approximate, and that a more detailed treatment should include the effect of a gate midway through the gorge, constituted by residues F330 and Y121. Nonetheless, the presence of F330 as a bottleneck in *Tc*AChE (Y337 in hAChE and mAChE) does not detract from our treatment, because this residue is known to be flexible (Harel et al., 1993). Moreover, in a recent MD study it was calculated that even if a putative gate made by F330 and Y121 is open for only 2.4% of the time, the transit of ACh will be slowed by no more than twofold (Zhou et al., 1998). In addition, we suggest that the aromatic side chain of F330 might play a more active role in assisting the clearance of cationic products from the gorge. In the F330A mutant, while k_{cat} for ACh is reduced, it is actually increased for its neutral analog, DBA (Ordentlich et al., 1993). A possible explanation for this observation is that substitution of a smaller side chain at position 330 widens the gorge, thus permitting faster traffic of the neutral product of DBA hydrolysis. In the case of Ch, however, removal of the aromatic side chain of F330 might destroy a shuttle-like mechanism for molecular traffic mediated by cation-π interactions between Ch and F330, thus reducing the rate of product clearance.

Our analysis of the contribution of long-range interactions to the binding of transition-state analogs of AChE

TABLE 6 Dependence on salt concentration of k_{cat} and comparison with calculated escape times

Theoretical		Experimental	
Potential (ϕ)	$\langle t\rangle$ (s)	k_{cat} (s^{-1})	
0 kT/e = 0 mV	$t_{min} = 3.3\times10^{-9}$	k_{max} 1.06×10^6 (I = 300 mM)*	k_{max} 0.58×10^6 (I = 500 mM)#
3.5 kT/e = −80 mv	$t_{max} = 13\times10^{-9}$	k_{min} 0.69×10^6 (I = 2 mM)*	k_{min} 0.20×10^6 (I = 5 mM)
Ratio	$t_{max}/t_{min} = 3.9$	$k_{max}/k_{min} = 4.3$	$k_{max}/k_{min} = 2.9$

*Nolte et al. (1980).
#Berman and Nowak (1992).

permits us to estimate whether the magnitude of these contributions might be sufficient to hinder the exit of Ch. The value of ~0.4 kcal/mol at $I = 145$ mM contributed by long-range electrostatic forces is close to the value of kT at 298.15K. Thus, it seems improbable that such a value would drastically impede Ch from drifting out of the active-site gorge by thermal diffusion. Ch is a noncompetitive inhibitor, with $K_i \approx 1.5$ mM at physiological salt concentration (Wilson and Alexander, 1962; Krupka, 1963; Eriksson and Augustinsson, 1979), and we can estimate the dissociation rate constant, k_{off}, from $K_i = k_{off}/k_{on}$. If k_{on} for Ch is comparable to the values for TFK^+ and NMA, which are around 10^9 M^{-1} s^{-1} for *Tc*AChE, then k_{off} will be ~10^6 s^{-1}. Thus, k_{off} for Ch is larger than k_{cat} (of which k_{off} is a component), which is in the range of 0.5–1 $\times$ 10^4 s^{-1}, by two orders of magnitude. Moreover, at low salt concentrations, k_{cat} values are decreased only by a fewfold, indicating that the binding strength of Ch is not significantly increased (Nolte et al., 1980; Hofer et al., 1984).

More evidence for the hypothesis that the potential gradient inside the active-site gorge of ChEs does not appreciably retard the clearance of positively charged products comes from studies of the ionic strength dependence of binding of TFK^+ (Quinn et al., 1995; Radic et al., 1997). These studies showed that k_{off} for TFK^+ is not dependent on salt concentration. This finding can be viewed in light of the fact that k_{on} and $1/K_i$, which are influenced by salt concentration, depend, respectively, on the free energy difference between the E + I state and the $EI^‡$ state, and between the E + I and the EI state. However, k_{off} depends on the energy difference between the EI and the $EI^‡$ states. Inspection of the free energy diagram displayed in Fig. 8 shows that if the effect of the electric field on the energies of EI and $EI^‡$ is of the same magnitude, the free energy barrier for release of the inhibitor will not be affected by the field. Hence, masking of the field by increasing salt concentration will have little influence on k_{off}.

There is some evidence pointing to the existence of alternative pathways for molecular traffic of substrates and products. A conformation for an open "back door" was suggested by molecular dynamics calculations (Gilson et al., 1994). However, a series of site-directed mutagenesis studies challenged this hypothesis by showing that mutations engineered to close the "back door" had little or no effect on the catalytic activity of AChE (Kronman et al., 1994; Faerman et al., 1996). Nonetheless, recent MD studies have revealed a number of possible alternative passageways to and from the active site (Wlodek et al., 1997b), and a MD study of the clearance from the gorge of acetic acid and acetate has identified a passageway for their release competing with the main entrance to the gorge (Enyedy et al., 1998). Furthermore, inspection of the crystal structure of *Tc*AChE carbamoylated by the physostigmine analog 8-(*cis*-2,6-dimethylmorpholino)octylcarbamoyleseroline has provided indirect experimental evidence for a "back door" (Bartolucci et al., 1999). In addition, a study on the binding of TFK^+ and TFK^0 to the complex of AChE with the PAS

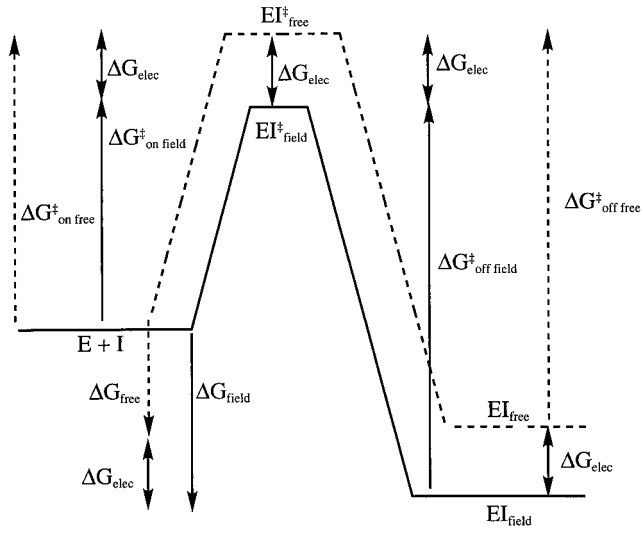

FIGURE 8 Free energy diagram for binding of TFK^+ to AChE in the presence and absence of an electrostatic field in the active-site gorge. ΔG is the total free energy difference between the E + I state (free enzyme and inhibitor) and the EI complex. $\Delta G^‡_{on}$ is the free energy difference between the E + I state and the activated binding state $EI^‡$, and $\Delta G^‡_{off}$ is the free energy difference between the EI complex and activated binding state $EI^‡$. The subscripts "field" and "free" refer, respectively, to the presence or absence of an electric field within the active-site gorge, and the difference in free energy due to this field is indicated by ΔG_{elec}. It can be seen that if ΔG_{elec} is the same for the $EI^‡$ state and for the EI complex, $\Delta G^‡_{off\ free} = \Delta G^‡_{off\ field}$. Consequently, k_{off}, which can be expressed as $k_{off} = \nu \exp(-\Delta G^‡_{off}/RT)$, according to transition state theory, will not be affected by the presence of an electric field within the gorge (Quinn et al., 1995).

inhibitor fasciculin II (FAS), a three-fingered polypeptide toxin from the venom of the green mamba (Karlsson et al., 1984), showed an increase in on rates for both TFK^+ and TFK^0 but diminished inhibition when W84, whose side chain is assumed to form a major part of the "back door," was mutated to Y, F, or A (Radic et al., 1995). FAS has been shown to bind in a "cork-and-bottle fashion" to the entrance of the active-site gorge of AChE (Bourne et al., 1995; Harel et al., 1995). The surface complementarity between enzyme and inhibitor is very large; ~2000 $Å^2$ of accessible surface is buried upon binding, and analysis of the accessible surface of the FAS-AChE complex shows that the route to the bottom of the gorge is blocked even for a 1-Å-radius probe.

From the above considerations, it can be concluded that side doors may exist in AChE, but rather than functioning as necessary exits for products, they might function as alternative routes for molecular traffic that are unmasked only when the principal pathway through the gorge is obstructed.

CONCLUSIONS

We have described a modular treatment for diffusion to and clearance from the active site of ChE and have estimated the contribution of a positive charge to the stabilization of the activated binding state of transition-state analogs for ChEs. Our model shows that diffusion of charged ligands relative

to neutral isosters is enhanced by ~10-fold, because of a surface trap for cationic ligands. A steering mechanism contributes a maximum of 20-fold to rate enhancement at low salt concentration, but only about twofold at physiological salt concentration. We identify D72 as the primary component of the surface trap, and residues D82 and D278 as supplementary components. The maximum contribution of a positive charge to the binding energy is calculated to be ~4.7 kcal M^{-1}, of which ~1.3 kcal M^{-1} can be attributed to long-range electrostatic contributions, and ~3.5 kcal M^{-1} to short-range electrostatic interactions. Employing absolute rate reaction theory, we calculate the electrostatic potential at the binding-site to be ~80 mV at zero ionic strength. The clearance of cationic products from the active-site gorge is considered as analogous to the escape of a particle from a 1D well in the presence of a linear potential. Our calculations and experimental data show that clearance of Ch via the main entrance of the gorge is not hindered by the active-site potential, and while alternative routes to the active site may exist, they do not seem to be required for optimal catalytic function of ChEs.

These findings allow us to hypothesize that ChEs may have evolved from an ancestor whose efficiency for hydrolyzing esters already approached the theoretical limit, as this property is still evident in the very efficient cleavage of neutral esters. The optimal catalytic efficiency of this putative ancestor was possibly due to the burying of the transition state in the heart of the protein, providing it with a preorganized polar environment (Fuxreiter and Warshel, 1998). The penalty paid for this arrangement is that diffusion to the active site is not as fast as that to a shallow cleft on the surface of the protein.

Our contention is that acceleration of diffusion for cationic esters in ChEs arose by evolution of two additional modules. The first module is a surface trap for cationic substrates at the entrance to the gorge, operating through short-range electrostatic interactions, whose effect is to raise the theoretical limit of diffusion to a buried active site by an order of magnitude. The second module is a steering effect by means of long-range electrostatic interactions, giving charged substrates an added edge of about one additional order of magnitude, with minimum hindrance to the molecular traffic of substrate and products. Optimal flow of substrates and products is ensured by the aromatic residues lining the gorge, which constitute a series of binding sites for quaternary ammonium moieties. These binding sites provide a method of orientation and stabilization of the substrate in the active site and possibly a shuttle-like mechanism for the clearance of products. Molecular "traffic jams" are averted by the affinity of these binding sites, because the strength of the cation-π interaction is strongly dependent on the mutual orientation of the groups involved and decreases sharply with distance.

The work we have presented shows that, in ChEs, maximum catalytic efficiency and specificity for a positively charged substrate are achieved by an optimal fine-tuning of long- and short-range electrostatic interactions, while at the same time striking a balance so that the electric potential inside the active site does not hinder the clearance of the positively charged product of the reaction.

The authors thank Drs. Charles Millard and Dan Quinn for valuable discussions. This work was supported by the U.S. Army Medical Research Acquisition Activity under Contract 17-97-2-7022; the Kimmelman Center for Biomolecular Structure and Assembly, Rehovot, Israel; and the Fourth Framework Program in Biotechnology of the European Union. IS is Bernstein-Mason Professor of Neurochemistry, and SAB is supported by the Theodore R. and Edlyn Racoosin Scholarship Fund.

REFERENCES

Adam, G., and M. Delbrück. 1968. Reduction of dimensionality in biological diffusion processes. *In* Structural Chemistry and Molecular Biology. A. Rich and N. Davidson, editors. Freeman, San Francisco. 198–215.

Allen, K. N., and R. H. Abeles. 1989a. Inhibition kinetics of acetylcholinesterase with fluoromethyl ketones. *Biochemistry.* 28:8466–8473.

Allen, K. N., and R. H. Abeles. 1989b. Inhibition of pig liver esterase by trifluoromethyl ketones: modulators of the catalytic reaction after inhibition kinetics. *Biochemistry.* 28:135–140.

Altschul, S. F., W. Gish, W. Miller, E. W. Myers, and D. J. Lipman. 1990. Basic local alignment search tool. *J. Mol. Biol.* 215:403–410.

Anthony, N., T. Rocheleau, G. Mocelin, H. J. Lee, and R. Ffrench-Constant. 1995. Cloning, sequencing and functional expression of an acetylcholinesterase gene from the yellow fever mosquito *Aedes aegypti*. *FEBS Lett.* 368:461–465.

Antosiewicz, J., M. K. Gilson, I. H. Lee, and J. A. McCammon. 1995a. Acetylcholinesterase: diffusional encounter rate constants for dumbbell models of ligand. *Biophys. J.* 68:62–68.

Antosiewicz, J., M. K. Gilson, and A. McCammon. 1994. Acetylcholinesterase: effects of ionic strength and dimerization on the rate constants. *Isr. J. Chem.* 34:151–158.

Antosiewicz, J., and J. A. McCammon. 1995. Electrostatic and hydrodynamic orientational steering effects in enzyme-substrate association. *Biophys. J.* 69:57–65.

Antosiewicz, J., J. A. McCammon, S. T. Wlodek, and M. K. Gilson. 1995b. Simulation of charge-mutant acetylcholinesterases. *Biochemistry.* 34: 4211–4219.

Antosiewicz, J., S. T. Wlodek, and J. A. McCammon. 1996. Acetylcholinesterase: role of the enzyme's charge distribution in steering charged ligands toward the active site. *Biopolymers.* 39:85–94.

Barak, D., A. Ordentlich, A. Bromberg, C. Kronman, D. Marcus, A. Lazar, N. Ariel, B. Velan, and A. Shafferman. 1995. Allosteric modulation of acetylcholinesterase activity by peripheral ligands involves a conformational transition of the anionic subsite. *Biochemistry.* 34:15444–15452.

Bartolucci, C., E. Perola, L. Cellai, M. Brufani, and D. Lamba. 1999. "Back door" opening implied by the crystal structure of a carbamoylated acetylcholinesterase. *Biochemistry.* 38:5714–5719.

Bataillé, S., P. Portalier, P. Coulon, and J. P. Ternaux. 1998. Influence of acetylcholinesterase on embryonic spinal rat motoneurones growth in culture: a quantitative morphometric study. *Eur. J. Neurosci.* 10: 560–572.

Bazelyansky, M., E. Robey, and J. F. Kirsch. 1986. Fractional diffusion-limited component of reactions catalyzed by acetylcholinesterase. *Biochemistry.* 25:125–130.

Bergmann, F., I. B. Wilson, and D. Nachmansohn. 1950. The inhibitory effect of stilbamidine, curare and related compounds and its relationship to the active groups of acetylcholine esterase. *Biochim. Biophys. Acta.* 6:217–224.

Berman, H. A., K. Leonard, and M. W. Nowak. 1991. Function of the peripheral anionic site of acetylcholinesterase. *In* Cholinesterases: Structure, Function, Mechanism, Genetics and Cell Biology. J. Massoulié, F. Bacou, E. Barnard, A. Chatonnet, B. P. Doctor, and D. M. Quinn, editors. American Chemical Society, Washington, DC. 229–234.

Berman, H. A., and M. W. Nowak. 1992. Influence of the ionic composition of the medium on acetylcholinesterase. *In* Multidisciplinary Ap-

proaches to Cholinesterase Functions. A. Shafferman and B. Velan, editors. Plenum Press, New York. 149–156.

Bhanumathy, C. D., and A. S. Balasubramanian. 1996. Evidence for a Zn(2+)-binding site in human serum butyrylcholinesterase. *Biochem. J.* 315:127–131.

Bourne, Y., P. Taylor, and P. Marchot. 1995. Acetylcholinesterase inhibition by fasciculin: crystal structure of the complex. *Cell.* 83:503–512.

Brady, K., T. C. Liang, and R. H. Abeles. 1989. pH dependence of the inhibition of chymotrypsin by a peptidyl trifluoromethyl ketone. *Biochemistry.* 28:9066–9070.

Changeux, J.-P. 1966. Responses of acetylcholinesterase from *Torpedo marmorata* to salts and curarizing drugs. *Mol. Pharmacol.* 2:369–392.

Chatonnet, A., and O. Lockridge. 1989. Comparison of butyrylcholinesterase and acetylcholinesterase. *Biochem. J.* 260:625–634.

Cousin, X., T. Hotelier, K. Giles, P. Lievin, J.-P. Toutant, and A. Chatonnet. 1997. The α/β fold family of proteins database and the cholinesterase genes server ESTHER. *Nucleic Acids Res.* 25:143–146.

Dawson, R. M., and H. D. Crone. 1973. Inorganic ion effects on the kinetic parameters of acetylcholinesterase. *J. Neurochem.* 21:247–249.

Dougherty, D. A. 1996. Cation-π interactions in chemistry and biology: a new view of benzene, Phe, Tyr and Trp. *Science.* 271:163–168.

Dougherty, D. A., and D. A. Stauffer. 1990. Acetylcholine binding by a synthetic receptor: implications for biological recognition. *Science.* 250: 1558–1560.

Enyedy, I. J., I. M. Kovach, and B. R. Brooks. 1998. Alternate pathways for acetic acid and acetate ion release from acetylcholinesterase: a molecular dynamics study. *J. Am. Chem. Soc.* 120:8043–8050.

Eriksson, H., and K. B. Augustinsson. 1979. A mechanistic model for butyrylcholinesterase. *Biochim. Biophys. Acta.* 567:161–173.

Faerman, C., D. Ripoll, S. Bon, Y. Le Feuvre, N. Morel, J. Massoulié, J. L. Sussman, and I. Silman. 1996. Site-directed mutants designed to test back-door hypotheses of acetylcholinesterase function. *FEBS Lett.* 386: 65–71.

Felder, C. E., S. A. Botti, S. Lifson, I. Silman, and J. L. Sussman. 1997. External and internal electrostatic potentials of cholinesterase models. *J. Mol. Graph. Mod.* 15:318–327.

Froede, H. C., and I. B. Wilson. 1971. Acetylcholinesterase. *In* The Enzymes. P. D. Boyer, editor. Academic Press, New York. 87–114.

Fuxreiter, M., and A. Warshel. 1998. Origin of the catalytic power of acetylcholinesterase: computer simulation studies. *J. Am. Chem. Soc.* 120:183–194.

Gilson, M. K., and B. Honig. 1988. Calculation of the total electrostatic energy of a macromolecular system: solvation energies, binding energies, and conformational analysis. *Proteins.* 4:7–18.

Gilson, M. K., T. P. Straatsma, J. A. McCammon, D. R. Ripoll, C. H. Faerman, P. H. Axelsen, I. Silman, and J. L. Sussman. 1994. Open "back door" in a molecular dynamics simulation of acetylcholinesterase. *Science.* 263:1276–1278.

Glasstone, S., K. J. Laidler, and H. Eyring. 1941. The Theory of Rate Processes. McGraw-Hill, New York.

Grauso, M., E. Culetto, D. Combes, Y. Fedon, J. P. Toutant, and M. Arpagus. 1998. Existence of four acetylcholinesterase genes in the nematodes *Caenorhabditis elegans* and *Caenorhabditis briggsae*. *FEBS Lett.* 424:279–284.

Haas, R., T. R. Marshall, and T. L. Rosenberry. 1992. Substrate-selective inhibition and peripheral site labeling of acetylcholinesterase by platinum(terpyridine)chloride. *In* Multidisciplinary Approaches to Cholinesterase Functions. A. Shafferman and B. Velan, editors. Plenum Press, New York. 131–140.

Harel, M., G. J. Kleywegt, R. B. G. Ravelli, I. Silman, and J. L. Sussman. 1995. Crystal structure of an acetylcholinesterase-fasciculin complex: interaction of a three-fingered toxin from snake venom with its target. *Structure.* 3:1355–1366.

Harel, M., D. M. Quinn, H. K. Nair, I. Silman, and J. L. Sussman. 1996. The x-ray structure of a transition state analog complex reveals the molecular origins of the catalytic power and substrate specificity of acetylcholinesterase. *J. Am. Chem. Soc.* 118:2340–2346.

Harel, M., I. Schalk, L. Ehret-Sabatier, F. Bouet, M. Goeldner, C. Hirth, P. H. Axelsen, I. Silman, and J. L. Sussman. 1993. Quaternary ligand binding to aromatic residues in the active-site gorge of acetylcholinesterase. *Proc. Natl. Acad. Sci. USA.* 90:9031–9035.

Harel, M., G. Kryger, J. L. Sussman, J. Silman, T. L. Rosenberry, W. D. Mallander, T. Lewis, R. J. Fletcher, and M. Guss. 1999. 3D structures of *Drosophila* acetylcholinesterase: implications for insecticide design. Abstracts IUCr XVII World Crystallography Congress, Glasgow, Scotland P09.04.023.

Hasan, F. B., J. L. Elkind, S. G. Cohen, and J. B. Cohen. 1981. Cationic and uncharged substrates and reversible inhibitors in hydrolysis by acetylcholinesterase: the trimethyl subsite (EC 3.1.1.7). *J. Biol. Chem.* 256:7781–7785.

Hasinoff, B. B. 1982. Kinetics of acetylthiocholine binding to electric eel acetylcholinesterase in glycerol/water solvents of increased viscosity. Evidence for a diffusion-controlled reaction. *Biochim. Biophys. Acta.* 704:52–58.

Hofer, P., U. P. Fringeli, and W. H. Hopff. 1984. Activation of acetylcholinesterase by monovalent (Na^+, K^+) and divalent (Ca^{2+}, Mg^{2+}) cations. *Biochemistry.* 23:2730–2734.

Honig, B., and A. Nicholls. 1995. Classical electrostatics in biology and chemistry. *Science.* 268:1144–1149.

Hosea, N. A., Z. Radic, I. Tsigelny, H. A. Berman, D. M. Quinn, and P. Taylor. 1996. Aspartate 74 as a primary determinant in acetylcholinesterase governing specificity to cationic organophosphonates. *Biochemistry.* 35:10995–11004.

Imperiali, B., and R. H. Abeles. 1986. Inhibition of serine proteases by peptidyl fluoromethyl ketones. *Biochemistry.* 25:3760–3767.

Inestrosa, N. C., A. Alvarez, C. A. Perez, R. D. Moreno, M. Vicente, C. Linker, O. I. Casanveva, C. Soto, and J. Garrido. 1996. Acetylcholinesterase accelerates assembly of amyloid beta-peptides into Alzheimer's fibrils: possible role of the peripheral site of the enzyme. *Neuron.* 16:881–891.

Jackson, S. E., and A. R. Fersht. 1993. Contribution of long-range electrostatic interactions to the stabilization of the catalytic transition state of the serine protease subtilisin BPN′. *Biochemistry.* 32:13909–13916.

Jones, S. A., C. Holmes, T. C. Budd, and S. A. Greenfield. 1995. The effect of acetylcholinesterase on outgrowth of dopaminergic neurons in organotypic slice culture of rat mid-brain. *Cell Tissue Res.* 279:323–330.

Karlsson, E., P. M. Mbugua, and D. Rodriguez-Ithurralde. 1984. Fasciculins, anticholinesterase toxins from the venom of the green mamba *Dendroaspis angusticeps. J. Physiol. (Paris).* 79:232–240.

Kortüm, G., and J. O. Bockris. 1951. Textbook of Electrochemistry. Elsevier Publishing, New York.

Kronman, C., A. Ordentlich, D. Barak, B. Velan, and A. Shafferman. 1994. The "back door" hypothesis for product clearance in acetylcholinesterase challenged by site-directed mutagenesis. *J. Biol. Chem.* 269: 27819–27822.

Krupka, R. M. 1963. The mechanism of action of acetylcholinesterase: substrate inhibition and the binding of inhibitors. *Biochemistry.* 2:76–82.

Laidler, K. J. 1965. Chemical Kinetics. McGraw-Hill, New York.

Layer, P. G., T. Weikert, and R. Alber. 1993. Cholinesterases regulate neurite growth of chick nerve cells *in vitro* by means of a non-enzymatic mechanism. *Cell Tissue Res.* 273:219–226.

Lifson, S., and J. Jackson. 1962. On the self diffusion of ions in a polyelectrolyte solution. *J. Chem. Phys.* 36:2410–2414.

Luhmer, M., K. Bartik, A. Dejaegere, P. Bovy, and J. Reisse. 1994. The importance of quadrupolar interactions in molecular recognition processes involving a phenyl group. *Bull. Soc. Chim. Fr.* 131:603.

Masson, P., M. T. Froment, C. F. Bartels, and O. Lockridge. 1996. Asp70 in the peripheral anionic site of human butyrylcholinesterase. *Eur. J. Biochem.* 235:36–48.

Masson, P., P. Legrand, C. F. Bartels, M. T. Froment, L. M. Schopfer, and O. Lockridge. 1997. Role of aspartate 70 and tryptophan 82 in binding of succinyldithiocholine to human butyrylcholinesterase. *Biochemistry.* 36:2266–2277.

Massoulié, J., L. Pezzementi, S. Bon, E. Krejci, and F.-M. Vallette. 1993. Molecular and cellular biology of cholinesterases. *Prog. Neurobiol.* 41:31–91.

Mendel, B., and H. Rudney. 1943. Studies on cholinesterase. 1. Cholinesterase and pseudo-cholinesterase. *Biochem. J.* 37:59–63.

Mutero, A., M. Pralavorio, V. Simeon, and D. Fournier. 1992. Catalytic properties of cholinesterases: importance of tyrosine 109 in *Drosophila* protein. *Neuroreport.* 3:39–42.

Nair, H. K., K. Lee, and D. M. Quinn. 1993. *m*-(*N,N,N,*-Trimethylammonio)trifluoroacetophenone: a femtomolar inhibitor of acetylcholinesterase. *J. Am. Chem. Soc.* 115:9939–9941.

Nair, H. K., J. Seravalli, T. Arbuckle, and D. M. Quinn. 1994. Molecular recognition in acetylcholinesterase catalysis: free-energy correlations for substrate turnover and inhibition by trifluoro ketone transition-state analogs. *Biochemistry.* 33:8566–8576.

Nolte, H. J., T. L. Rosenberry, and E. Neumann. 1980. Effective charge on acetylcholinesterase active sites determined from the ionic strength dependence of association rate constants with cationic ligands. *Biochemistry.* 19:3705–3711.

Ordentlich, A., D. Barak, C. Kronman, N. Ariel, Y. Segall, B. Velan, and A. Shafferman. 1996. The architecture of human acetylcholinesterase active center probed by interactions with selected organophosphate inhibitors. *J. Biol. Chem.* 271:11953–11962.

Ordentlich, A., D. Barak, C. Kronman, Y. Flashner, M. Leitner, Y. Segall, N. Ariel, S. Cohen, B. Velan, and A. Shafferman. 1993. Dissection of the human acetylcholinesterase active center determinants of substrate specificity. Identification of residues constituting the anionic site, the hydrophobic site, and the acyl pocket. *J. Biol. Chem.* 268:17083–17095.

Peitsch, M. C. 1996. ProMod and Swiss-Model: Internet-based tools for automated comparative protein modelling. *Biochem. Soc. Trans.* 24: 274–279.

Porschke, D., C. Créminon, X. Cousin, C. Bon, J. Sussman, and I. Silman. 1996. Electrooptical measurements demonstrate a large permanent dipole moment associated with acetylcholinesterase. *Biophys. J.* 70: 1603–1608.

Quinn, D. M. 1987. Acetylcholinesterase: enzyme structure, reaction dynamics, and virtual transition states. *Chem. Rev.* 87:955–979.

Quinn, D. M., J. Serravalli, H. K. Nair, R. Medhekar, B. Husseini, Z. Radic, D. C. Vellom, N. Pickering, and P. Taylor. 1995. The function of electrostatics in acetylcholinesterase catalysis. *In* Enzymes of the Cholinesterase Family. D. M. Quinn, A. S. Balasubramanian, B. P. Doctor, and P. Taylor, editors. Plenum Press, New York. 203–207.

Radic, Z., P. D. Kirchoff, D. M. Quinn, J. A. McCammon, and P. Taylor. 1997. Electrostatic influence on the kinetics of ligand binding to acetylcholinesterase. *J. Biol. Chem.* 272:23265–23277.

Radic, Z., N. A. Pickering, D. C. Vellom, S. Camp, and P. Taylor. 1993. Three distinct domains in the cholinesterase molecule confer selectivity for acetyl- and butyrylcholinesterase inhibitors. *Biochemistry.* 32: 12074–12084.

Radic, Z., D. M. Quinn, D. C. Vellom, S. Camp, and P. Taylor. 1995. Allosteric control of acetylcholinesterase catalysis by fasciculin. *J. Biol. Chem.* 270:20391–20399.

Radic, Z., E. Reiner, and P. Taylor. 1991. Role of the peripheral anionic site on acetylcholinesterase: inhibition by substrates and coumarin derivatives. *Mol. Pharmacol.* 39:98–104.

Ripoll, D. R., C. H. Faerman, P. H. Axelsen, I. Silman, and J. L. Sussman. 1993. An electrostatic mechanism for substrate guidance down the aromatic gorge of acetylcholinesterase. *Proc. Natl. Acad. Sci. USA.* 90:5128–5132.

Rosenberry, T. L. 1975a. Acetylcholinesterase. *Adv. Enzymol.* 43:103–218.

Rosenberry, T. L. 1975b. Catalysis by acetylcholinesterase: evidence that the rate-limiting step by acetylation with certain substrate precedes general acid-base catalysis. *Proc. Natl. Acad. Sci. USA.* 72:3834–3838.

Rosenberry, T. L., and E. Neumann. 1977. Interaction of ligands with acetylcholinesterase. Use of temperature-jump relaxation kinetics in the binding of specific fluorescent ligands. *Biochemistry.* 16:3870–3877.

Samson, R., and J. M. Deutch. 1978. Diffusion-controlled reaction to a buried active site. *J. Chem. Phys.* 68:285–290.

Schalk, I., L. Ehret-Sabatier, F. Bouet, M. Goeldner, and C. Hirth. 1992. Structural analysis of acetylcholinesterase ammonium binding sites. *In* Multidisciplinary Approaches to Cholinesterase Functions. A. Shafferman and B. Velan, editors. Plenum Press, New York. 117–120.

Shafferman, A., A. Ordentlich, D. Barak, C. Kronman, R. Ber, T. Bino, N. Ariel, R. Osman, and B. Velan. 1994. Electrostatic attraction by surface charge does not contribute to the catalytic efficiency of acetylcholinesterase. *EMBO J.* 13:3448–3455.

Shafferman, A., B. Velan, A. Ordentlich, C. Kronman, H. Grosfeld, M. Leitner, Y. Flashner, S. Cohen, D. Barak, and N. Ariel. 1992. Substrate inhibition of acetylcholinesterase: residues affecting signal transduction from the surface to the catalytic center. *EMBO J.* 11:3561–3568.

Sitkoff, D., K. A. Sharp, and B. Honig. 1994. Accurate calculation of hydration free energies using macroscopic solvent models. *J. Phys. Chem.* 98:1978–1988.

Smissaert, H. R. 1981. Acetylcholinesterase: evidence that sodium ion binding at the anionic site causes inhibition of the second-order hydrolysis of acetylcholine and a decrease of its pKa as well as of deacetylation. *Biochem. J.* 197:163–170.

Srivatsan, M., and B. Peretz. 1997. Acetylcholinesterase promotes regeneration of neurites in cultured adult neurons of *Aplysia. Neuroscience.* 77:921–931.

Stauffer, D. A., and A. Karlin. 1994. Electrostatic potential of the acetylcholine binding sites in the nicotinic receptor probed by reactions of binding-site cysteines with charged methanethiosulfonates. *Biochemistry.* 33:6840–6849.

Sunner, J., K. Nishizawa, and P. Kebarle. 1981. Ion-solvent molecule interactions in the gas phase. *J. Phys. Chem.* 85:1815–1820.

Sussman, J. L., M. Harel, F. Frolow, C. Oefner, A. Goldman, L. Toker, and I. Silman. 1991. Atomic structure of acetylcholinesterase from *Torpedo californica:* a prototypic acetylcholine-binding protein. *Science.* 253: 872–879.

Takahashi, L. H., R. Radhakrishnan, R. E. Rosenfield, Jr., E. F. Meyer, Jr., D. A. Trainor, and M. Stein. 1988. X-ray diffraction analysis of the inhibition of porcine pancreatic elastase by a peptidyl trifluoromethylketone. *J. Mol. Biol.* 201:423–428.

Tan, R. C., T. N. Truong, J. A. McCammon, and J. L. Sussman. 1993. Acetylcholinesterase: electrostatic steering increases the rate of ligand binding. *Biochemistry.* 32:401–403.

Taylor, P., and S. Lappi. 1975. Interaction of fluorescence probes with acetylcholinesterase. The site and specificity of propidium. *Biochemistry.* 14:1989–1997.

Taylor, P., and Z. Radic. 1994. The cholinesterases: from genes to proteins. *Annu. Rev. Pharmacol. Toxicol.* 34:281–320.

Toutant, J. P. 1989. Insect acetylcholinesterase: catalytic properties, tissue distribution and molecular forms. *Prog. Neurobiol.* 32:423–446.

Vellom, D. C., Z. Radic, Y. Li, N. A. Pickering, S. Camp, and P. Taylor. 1993. Amino acid residues controlling acetylcholinesterase and butyrylcholinesterase specificity. *Biochemistry.* 32:12–17.

Warwicker, J., and H. C. Watson. 1982. Calculation of the electric potential in the active site cleft due to alpha-helix dipoles. *J. Mol. Biol.* 157: 671–679.

Willbold, E., and P. G. Layer. 1994. Butyrylcholinesterase regulates laminar retinogenesis of the chick embryo *in vitro. Eur. J. Cell Biol.* 64:192–199.

Wilson, I. B., and J. Alexander. 1962. Acetylcholinesterase: reversible inhibitors, substrate inhibition. *J. Biol. Chem.* 237:1323–1326.

Wilson, I. B., and F. Bergmann. 1950. Studies on cholinesterase. VII. The active surface of acetylcholine esterase derived from effects of pH on inhibitors. *J. Biol. Chem.* 185:479–489.

Wlodek, S. T., J. Antosiewicz, and J. M. Briggs. 1997a. On the mechanism of acetylcholinesterase action: the electrostatically induced acceleration of the catalytic step. *J. Am. Chem. Soc.* 119:8159–8165.

Wlodek, T. S., T. W. Clark, L. R. Scott, and A. J. McCammon. 1997b. Molecular dynamics of acetylcholinesterase dimer complexed with tacrine. *J. Am. Chem. Soc.* 119:9513–9522.

Zhou, H. X., J. M. Briggs, and J. A. McCammon. 1996. A 240-fold electrostatic rate enhancement for acetylcholinesterase substrate binding can be predicted by the potential within the active site. *J. Am. Chem. Soc.* 118:13069–13070.

Zhou, H. X., S. T. Wlodek, and J. A. McCammon. 1998. Conformational gating as a mechanism for enzyme specificity. *Proc. Natl. Acad. Sci. USA.* 95:9280–9283.

Zhu, K. Y., and J. M. Clark. 1995. Cloning and sequencing of a cDNA encoding acetylcholinesterase in Colorado potato beetle, *Leptinotarsa decemlineata* (Say). *Insect Biochem. Mol. Biol.* 25:1129–1138.